# REACTOR CORE MATERIALS

*A Quarterly Technical Progress Review*

Prepared for U. S. ATOMIC ENERGY COMMISSION by BATTELLE MEMORIAL INSTITUTE

4 - DEC 15
Copy 1959

*November 1959*

VOLUME 2

NUMBER 4

# TECHNICAL PROGRESS REVIEWS

To meet the needs of industry for concise summaries of current atomic developments, the Atomic Energy Commission is publishing this series, Technical Progress Reviews. Issued quarterly, each of the reviews digests and evaluates the latest findings in a specific area of nuclear technology and science.

The four journals published in this series are:

*Nuclear Safety*, W. B. Cottrell, editor, R. A. Charpie, advisory editor, and associates, Oak Ridge National Laboratory

*Power Reactor Technology*, Walter H. Zinn and associates, General Nuclear Engineering Corporation

*Reactor Core Materials* (covering solid material developments), R. W. Dayton, E. M. Simons, and associates, Battelle Memorial Institute

*Reactor Fuel Processing*, Stephen Lawroski and associates, Chemical Engineering Division, Argonne National Laboratory

Each journal may be purchased ($2.00 per year for subscription and individual issues $0.55) from the Superintendent of Documents, U. S. Government Printing Office, Washington 25, D. C. See back cover for remittance instructions and foreign postage requirements.

●

## Availability of Reports Cited in This Review

*Unclassified AEC reports* are available for inspection at AEC depository libraries and are sold by the Office of Technical Services, Department of Commerce, Washington 25, D..C.

*Unclassified reports issued by other Government agencies or private organizations* should be requested from the originator.

*Unclassified British and Canadian reports* may be inspected at AEC depository libraries. British reports are sold by the British Information Service, 45 Rockefeller Plaza, New York, N. Y.; Canadian reports (AECL series) are sold by the Scientific Document Distribution Office, Atomic Energy of Canada, Ltd., Chalk River, Ontario, Canada.

*Classified U. S. and foreign reports* identified in this journal as Secret or Confidential may be purchased by properly cleared Access Permit Holders from the Technical Information Service Extension, U. S. Atomic Energy Commission, P. O. Box 1001, Oak Ridge, Tenn. Such reports may be inspected at classified AEC depository libraries.

# REACTOR CORE MATERIALS

## A REVIEW OF RECENT DEVELOPMENTS

Prepared for U. S. ATOMIC ENERGY COMMISSION
by BATTELLE MEMORIAL INSTITUTE

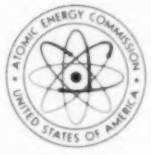


● NOV. 1959

● VOLUME 2

● NUMBER 4

# *foreword*

This issue marks the completion of the second year of publication of *Reactor Core Materials*, one of a group of Technical Progress Reviews prepared at the request of the Industrial Information Branch of the U. S. Atomic Energy Commission. Each quarter, staff members of Battelle Memorial Institute comb the literature for new developments and significant findings in designated areas of technology and write these up in the form of annotated reviews. The compilation includes four sections organized by function (fuels, moderators, poisons, and structural materials) and a fifth section devoted to fabrication techniques which are important in reactor-core manufacture.

The intended audience falls into two categories: (1) those who wish to keep abreast of developments in a general way and (2) specialists who are interested in the details of advances in specific areas. Since this type of publication cannot hope to present more than the highlights of current work in the vast field covered, readers in the latter category will find the extensive bibliographic reference list at the end of each section useful for locating sources of more detailed information in particular areas.

R. W. DAYTON
E. M. SIMONS
*Battelle Memorial Institute*

# *contents*


| | | |
|---|---|---|
| ii | | Foreword |
| 1 | I | FUEL AND FERTILE MATERIALS |
| 1 | | Unalloyed Uranium |
| 2 | | Alpha-Uranium Alloys |
| 2 | | Gamma-phase Alloys |
| 3 | | Dilute Uranium Alloys |
| 5 | | Plutonium and Its Alloys |
| 5 | | Thorium and Its Alloys |
| 7 | | Refractory Fuel and Fertile Materials |
| 9 | | Mechanism of Corrosion of Fuel Alloys |
| 9 | | Basic Studies of Radiation Effects in Fuel Materials |
| 11 | | References |
| 14 | II | MODERATOR MATERIALS |
| 14 | | Graphite |
| 14 | | Beryllium Metal and Alloys |
| 15 | | Solid Hydrides |
| 16 | | References |
| 17 | III | NUCLEAR POISONS |
| 17 | | Boron-containing Dispersions |
| 19 | | References |
| 20 | IV | CLADDING AND STRUCTURAL MATERIALS |
| 20 | | Corrosion |
| 24 | | Zirconium-Water Reactions |
| 25 | | Radiation Effects in Nonfuel Materials |
| 30 | | Selected Metallurgical Aspects of Cladding and Structural Materials |
| 34 | | Selected Mechanical Properties of Cladding and Structural Materials |
| 38 | | References |
| 41 | V | SPECIAL FABRICATION TECHNIQUES |
| 41 | | Melting, Casting, Heat-treatment, and Hot Working |
| 42 | | Cladding |
| 44 | | Welding and Brazing |
| 44 | | Nondestructive Testing |
| 45 | | References |


Issued quarterly by the U. S. Atomic Energy Commission. Use of funds for printing this publication approved by the Director of the Bureau of the Budget on November 1, 1957.

# REACTOR CORE MATERIALS

## *FUEL AND FERTILE MATERIALS*

### *Unalloyed Uranium*

Argonne[1] has studied preferred orientation in recrystallized high-purity uranium rod, rolled to an 85 per cent reduction at 300°C. The as-rolled texture could be described as a duplex (0 4 1) and (3 5 2), with the (0 4 1) being the major component and with considerable spread about each component. The recrystallized rod showed approximate (0 4 1) and (3 9 2) components with considerable spread. Another investigation[2] deals with recrystallization of uranium sheet that had been rolled to 80 per cent reduction in thickness at room temperature. Three different preferred orientations could be developed upon recrystallization. One preferred orientation, which is essentially the same as that of the as-rolled material, resulted from annealing for long times at 360°C or at lower temperatures; a second was created by annealing for moderate times between 400 and 600°C; and the third accompanied grain coarsening at 650°C. The microstructures of the as-rolled and annealed specimens were extremely heterogeneous because of the large grain size prior to final fabrication at room temperature. The as-rolled structures consisted of heavily deformed areas and smaller quantities of lightly deformed material. The annealing of the heavily deformed areas was characterized by initial creation of very fine recrystallized grains which were absorbed later by discontinuous growth of larger grains. Lightly deformed areas, upon annealing, first exhibited recovery by polygonization and then underwent normal recrystallization.

In another program[3] the effect of transfer time from the beta heat-treating bath to the quench medium on the recrystallization of beta-quenched uranium was of interest. A critical transfer time which relates to the time required to immerse samples from a temperature above the beta-alpha transformation in a quench medium directly affects the beta-cooled structure and its ease of recrystallization upon alpha-phase annealing. Within the critical transfer time, the ease of recrystallization and the degree of grain refinement of beta-cooled samples are superior to those of samples quenched beyond the critical transfer time.

Preliminary experiments have been conducted on the irradiation cycling and partial beta-phase irradiation of uranium.[4] In this investigation, some of the uranium specimens were irradiated continuously, whereas others were cycled in and out of the reactor. Although most of the specimens were entirely in the alpha phase during irradiation, some were irradiated so that their centers were above alpha-phase temperatures. Both highly textured material (300°C rolled) and nominally randomly oriented material (300°C rolled and beta quenched) were studied. It appeared that irradiation cycling of both types of materials produced greater elongations than would be anticipated on the assumption that the effects of irradiation and thermal cycling acting alone were additive. The material rolled at 300°C showed no external effects due to central irradiation temperatures being above those limiting the alpha phase. However, beta-quenched material, which was irradiated so that central temperatures were above those required for stability of the alpha phase, developed severe distortions which were greater under cycling conditions. It was also noted that uranium rolled at 300°C began to elongate under irradiation at burn-ups as low as 0.0002 at.% (2 Mwd/ton).

British investigators[5] have shown that alpha-uranium deformation at 450°C is very similar to the deformation characteristics at room temperature; that is, twinning is prevalent. At 500°C, twinning is much decreased and there is some evidence for pencil glide in a (1 1 0) direction. There could be three reasons for this, namely, the occurrence of additional slip modes,

grain-boundary slip, and the relative decrease of the critical shear stress for slip compared to twinning.

Kinetics of the reaction of steam with unalloyed uranium at 160 to 1060°C and 1 atm pressure were determined by the British.[6] Up to 880°C the reaction follows a linear rate. Above this temperature a parabolic rate law applies for the first 60 to 120 min, after which corrosion is linear; the oxide formed in the initial period gives protection to the underlying metal, and the subsequent linear rate is as low as that at 200°C. X-ray diffraction of the reaction product indicates that $UO_2$ is formed over almost the whole temperature range.

The elastic moduli of polycrystalline uranium were calculated[7] from single-crystal data by two different methods and were compared with measured values. The values obtained for $E$ (Young's modulus) were 30.5 and $28.3 \times 10^6$ psi; values obtained for $G$ (shear modulus) were 12.77 and $11.69 \times 10^6$ psi.

The structure of a vacuum-deposited film of uranium was studied by means of electron microscopy and electron diffraction.[8] The results show that the uranium in the thin film assumes the beta-phase structure.

Of general interest are recently published books containing information on the metallurgy of uranium[9] and the chemistry of uranium.[10]

(M. S. Farkas)

## *Alpha-uranium Alloys*

Constitution of low-carbon alloys of the uranium-carbon system is reported by Argonne.[11] A eutectic point was found at 0.98 at.% carbon at 1116.6°C, and two eutectoid reactions, alpha uranium ⇌ beta uranium + UC and beta uranium ⇌ alpha uranium + UC, at 771.8 and 665.9°C, respectively, or 3.0 and 1.8°C below the transformation temperatures of the pure metal. The solubility of carbon in gamma uranium decreases from 0.30 ± 0.075 at.% at the eutectic temperature to 0.09 ± 0.04 at.% at the eutectoid temperature. The beta and alpha solubilities for carbon are about 10 and 3 ppm, respectively.

Atomics International[12] reports on the evaluation of the as-cast properties of uranium–3.5 wt.% molybdenum, uranium–3.5 wt.% molybdenum–0.5 wt.% silicon, uranium–3.5 wt.% molybdenum–0.5 wt.% aluminum, and uranium–2 wt.% zirconium–0.1 wt.% aluminum. These alloys were evaluated by means of mechanical-property and thermal-cycling tests to determine reference alloys for the OMR (Organic Moderated Reactor). The uranium–3.5 wt.% molybdenum and uranium–3.5 wt.% molybdenum–0.5 wt.% silicon alloys were found to be the best performers.

In a recent British report,[13] data on the solubility and diffusion of hydrogen in uranium are reviewed. In addition, a study is presented of the behavior of hydrogen in uranium specimens containing different amounts of carbon, after hydrogenation at various temperatures, at hydrogen pressures varying from 1 to 130 atm. The precipitation of beta $UH_3$ during cooling after these treatments and the decomposition during subsequent vacuum annealing were studied metallographically. No microscopic evidence of voids was found as a result of the decomposition of hydride particles. During hydrogenation above 800°C and at high pressures, new hydrogen-rich phases were obtained in pure uranium and in uranium containing carbon. In the carbon-bearing material the new phase was found to have the approximate composition $U_3CH_5$. In the pure uranium the new hydride phase formed was not identified.

Grain refinement of uranium by means of alloy additions is discussed in a paper recently published by the French.[14] (M. S. Farkas)

## *Gamma-phase Alloys*

Harwell[15] reports that the gamma phase can be rendered metastable under critical cooling conditions in uranium alloys with additions of approximately 10 at.% titanium, niobium, zirconium, or molybdenum. The metastable phase can then transform by a shear mechanism to form characteristic banded structures or by nucleation and growth to form equiaxed grains. The decomposition structures with differing metallographic appearances give similar X-ray patterns designated as "distorted alpha," since the patterns correspond to a contraction in the $b$ direction of the normal orthorhombic alpha cell. The formation of these metastable structures is apparently dependent upon composition, cooling rate, and effect of the solute element on the incubation period and decomposition rate of the gamma phase.

A study of transformation kinetics in a series of gamma-phase alloys is under way at Bettis.[16] Correlation between dilatometric and hardness data is reported to be good, but correlation of these with metallographic data is erratic.

### Uranium-Niobium

The results of a study of the constitution of uranium-niobium alloys are reported by Harwell.[17] The phase diagram given is in good general agreement with that reported by U. S. investigators.

Concentration-penetration curves for diffusion in uranium-niobium couples at 700, 900, 925, and 1000°C are shown in a Battelle report.[18] At 1000°C the curve shows a smooth variation in composition with distance, whereas, at the lower temperatures, breaks in the curves, reflecting the gamma-immiscibility gap, are observed. Based on the compositions at which these breaks occur, a two-phase region extending from 40 to 60 at.% uranium at 925°C, from 35 to 65 at.% uranium at 900°C, and from 24 to 80 at.% uranium at 700°C is indicated.

Studies of the gamma-phase reversion phenomenon in uranium-niobium alloys are in progress at Bettis.[16] Postirradiation electrical-resistivity measurements and X-ray diffraction examinations are in progress.

### Uranium-Molybdenum

In a study of the transformation of uranium-molybdenum alloys, Harwell reports[19] that, in quenched 5 and 10 at.% molybdenum alloys, different forms of distorted alpha occur and that, in a 15 at.% molybdenum alloy, a distorted anisotropic phase based on the gamma-uranium cell occurs. In the 25 and 30 at.% molybdenum alloys, gamma is retained on quenching. Transformation of the metastable structures in the 5, 10, and 15 at.% alloys is accompanied by a marked hardness increase, whereas transformation of the 25 and 30 at.% alloys was found to be accompanied by only minor hardness changes. The appearance of the alpha-uranium phase in the 25 at.% alloy after heat-treatments at 550°C for over 100 days supports the U. S. interpretation of the uranium-molybdenum phase diagram, in which a very limited solid-solution range to the intermediate delta-phase region is indicated.

A study of the oxidation of uranium-molybdenum alloys containing up to 15.5 wt.% molybdenum in $CO_2$ at 500 to 1000°C and in air at 500 to 900°C is also reported by Harwell.[20] Molybdenum decreased oxidation rates of uranium in $CO_2$ at 800 to 1000°C and in air at 500 to 680°C by factors of up to 140, but increased them in $CO_2$ at 500 to 680°C by factors of up to 8. At a particular temperature, the particle size of the oxidation product decreased as the oxidation rate increased; sintering normally accompanied the reductions in rate.

A French paper[21] provides a summary of uranium-molybdenum alloy behavior with some discussion of the uranium-molybdenum system. The systems are discussed from the viewpoint of possible application as gamma-phase fuels in a $CO_2$-cooled reactor.

### Uranium-Titanium

Harwell reports[22] that the gamma phase of the uranium-titanium system may decompose on quenching to one of three metastable phases. On mercury quenching a 10 at.% alloy, the alloy undergoes a shear transformation to form a distorted alpha structure. In a 15 at.% alloy a highly stressed, slightly anisotropic form of gamma occurs on quenching, and at slower cooling rates a distorted form of alpha occurs by a nucleation and growth process. On mercury quenching a 20 at.% alloy, gamma is retained. Hardness increases associated with the formation of $U_2Ti$ are noted at slower cooling rates.

(A. A. Bauer)

## *Dilute Uranium Alloys*

### Aluminum-Uranium Alloys

Continued studies by Battelle[23] of aluminum-uranium alloys modified with 3 wt.% additions of either tin or zirconium still indicate that these additions generally improve the binary alloy. Although the ultimate strength of the extruded ternary alloys is slightly below that for the extruded binary, the ductility is improved by the ternary addition. A comparison of the

strength and ductility of both cast and extruded material appears below.

| Ternary addition to Al–35 wt.% U alloy, wt.% | Ultimate strength, psi | | Reduction of area, % | |
|---|---|---|---|---|
| | Cast | Extruded | Cast | Extruded |
| None | 17,000 | 21,500 | 2.35 | 1.85 |
| 3 tin | 19,000 | 17,900 | 4.34 | 3.5 |
| 3 zirconium | 19,600 | 17,000 | 3.75 | 3.62 |
| 3 silicon | 12,500 | 22,000 | 3.5 | 3.75 |

Probably a more important property of the tin and zirconium ternary alloys is the fact that an extrusion pressure of only 9.37 tsi was needed to form them, whereas 12.2 tsi was needed to form the binary alloy and the silicon-containing ternary.

The French[24] report some interesting results obtained from a study of the preparation of aluminum-uranium alloys by reduction of a uranium salt in an aluminum bath. Small batches of aluminum–25 wt.% uranium alloys were prepared by reducing $UF_4$ with lithium in a bath of molten aluminum. A combination of 198 g of $UF_4$ + 17 g of lithium + 517.4 g of aluminum gave uranium recoveries of 99 per cent in the form of alloy. Some success was also attained with sodium; however, a combination of 198 g of $UF_4$ + 58 g of sodium + 479 g of aluminum gave a recovery of only 92.2 per cent.

## Zirconium-Uranium Alloys

The British[25] have used both in-pile and out-of-pile heating experiments to study the release of fission gas from a zirconium–5 wt.% highly enriched uranium alloy. For the in-pile test a small specimen was suspended by a platinum wire in a silica cell surrounded by an electrically heated furnace. This arrangement produced specimen temperatures up to 1000°C during irradiation. The fission gases were swept from the furnace by a helium carrier to a counting chamber, where $Xe^{135}$, $Kr^{85}$, and $Xe^{133}$ were determined by a gamma-scintillation meter. Prior to the out-of-pile tests the specimens were irradiated for 84 hr at 80°C (reactor ambient temperature) and cooled for 7 days. These specimens were then checked for $Xe^{133}$ release at room temperature, 200, 400, and 600°C.

A study of the in-pile test data shows that the fission gas released at temperatures below 600°C was due solely to the contribution of fission recoil. Above 600°C the rapidity of gas release was due to diffusion. The diffusion coefficients (in square centimeters per second) for the rare gases in the zirconium–5 wt.% uranium were derived from this work and are listed below.

| Temp., °C | Diffusion coefficient ($D$), $cm^2/sec$ | | |
|---|---|---|---|
| | $Xe^{135}$ | $Kr^{185}$ | $Xe^{133}$ |
| 700 | $2.5 \times 10^{-12}$ | $1.8 \times 10^{-12}$ | $2.6 \times 10^{-13}$ |
| 800 | $8.7 \times 10^{-12}$ | $4.6 \times 10^{-12}$ | $8.0 \times 10^{-13}$ |
| 900 | $1.9 \times 10^{-11}$ | $7.6 \times 10^{-12}$ | $1.5 \times 10^{-12}$ |

The out-of-pile tests resulted in no release at room temperature and only a small release at 200 and 400°C. This release is probably due to grain-boundary diffusion or minute surface cracks but certainly not bulk diffusion. At 600°C and above, the release of gas increases sharply, with the rate of release increasing with temperature. Thus it can be said that above 600°C bulk diffusion is the mechanism which controls fission-gas release from the zirconium–5 wt.% uranium alloy.

Bettis has prepared a résumé of available data on zirconium-dilute uranium alloys. The evaluation of the compiled data on binary alloys containing 3 to 22 wt.% uranium and from 0 to 0.113 wt.% $B^{10}$ which were irradiated to burn-ups of 1.9 total at.% indicates that irradiation-induced swelling accounts for a volume change of 7 per cent or less per at.% burn-up at temperatures up to 800°F; above this temperature swelling increases rapidly. In the case of post-irradiation annealing, uniform swelling of 5 to 6 per cent per at.% burn-up occurs with specimens having burn-ups up to 1.4 at.% when the annealing temperature is below 950°F. Other data indicate that if the burn-up exceeds 1.5 total at.%, a 900°F postirradiation anneal will cause gross swelling (20 per cent per at.% burn-up and over).

It is also pointed out that something significant happens to the metal structures of zirconium-uranium-boron alloys between 1.5 and 2.0 total at.% burn-up. This is based on the changes in swelling and corrosion behavior which occur after such burn-ups. It is possible that lattice changes occur at this point or that there is a critical concentration of fission products which is reacted at about this burn-up. Swelling can be predicted by calculations based on burn-up, irradiation temperature, yield point, and creep

rate. The swelling rate varies directly with yield point and the cube root of the creep rate. Therefore a logical first step in increasing resistance to radiation-induced swelling is to increase the yield point of the material. This could provide an increase in the irradiation life of the material.

### Niobium-Uranium Alloys

Binary alloys of niobium and uranium containing from 10 to 50 wt.% uranium are being exposed to a number of different environments at Battelle.[18,26] The resistance of all the alloys to corrosion by 600°F water after a 7-day exposure is about the same as that of unalloyed niobium (weight gain of between 0.18 and 0.29 mg/cm$^2$), whereas the weight gain after 7 days in 680°F water was higher (between 0.28 and 1.8 mg/cm$^2$). There was no apparent correlation with composition. The same alloys after exposure for 500 hr to 572°F air maintained an adherent film which allowed them to show a reasonable resistance (weight gain of between 0.28 and 0.40 mg/cm$^2$). On the other hand, exposures to air at 662°F for 60 hr resulted in weight losses of 2 to 6 mg/cm$^2$ for all alloys except the 10 wt.% uranium, which exhibited a loss of 1.0 mg/cm$^2$. Exposures for 60 hr to 752°F air resulted in weight gains of between 12 and 20 mg/cm$^2$. A 50-hr exposure in $CO_2$ at 600°F resulted in the formation of a spalling oxide which accounted for a weight change of about 0.2 mg/cm$^2$ for the 10 and 20 wt.% uranium alloys and a change of about 0.35 mg/cm$^2$ for the other alloys. Interesting tensile data obtained at room temperature and at 1600°F are shown in Table I-1.

Table I-1 TENSILE DATA FOR NIOBIUM-URANIUM ALLOYS

| U content, wt.% | Impurity content, ppm | | Ultimate tensile strength, psi | | Reduction of area, % | |
|---|---|---|---|---|---|---|
| | O | Zr | RT | 1600°F | RT | 1600°F |
| 10 | 700 | 0.17 | 70,000 | 51,000 | 11 | 12 |
| | 300 | 0.02 | 77,900 | | | |
| | 600 | 0.74 | | 49,500 | | 31 |
| 20 | 300 | 0.02 | 102,000 | 68,400 | 21 | 0 |
| | 600 | 0.74 | 95,500 | 71,000 | 19 | 16 |
| 30 | 600 | 0.74 | | 71,200 | | 0 |

Although mechanical-property data are sparse, it is obvious that these materials have high strengths at both room and elevated temperatures.

### Miscellaneous Alloys

Sylvania-Corning[27] is studying dispersions of uranium in a matrix of yttrium or yttrium alloy as a fuel which may have potential value as a stable material under high-temperature conditions of irradiation. Dispersions containing 5, 25, 50, 65, and 85 wt.% uranium have been prepared and examined. The following conclusions have been reached as a result of the work done thus far:

1. An increase in uranium content increases room-temperature hardness; however, the hardness decreases rapidly at high temperature with increased uranium content.
2. The size of the uranium particles makes no difference in tensile properties; however, the smaller the yttrium particles the greater is the tensile strength.
3. Distortion caused by cycling in the alpha range occurs in dispersions containing greater than 65 wt.% uranium; below 65 wt.%, essentially no distortion occurs. (R. F. Dickerson)

## *Plutonium and Its Alloys*

### Plutonium-Zinc Alloys

A tentative plutonium-zinc phase diagram determined at Los Alamos[29] shows four intermetallic compounds: $PuZn_2$, $Pu_2Zn_9$, $PuZn_8$, and $Pu_2Zn_{17}$. A eutectic occurring at about 830°C has been established between $PuZn_2$ and $Pu_2Zn_9$. Eutectic composition is about 74 at.% zinc. Temperature of peritectic melting of $Pu_2Zn_{17}$ was determined to be about 810°C and that of $PuZn_8$ about 880°C. (V. W. Storhok)

## *Thorium and Its Alloys*

A *Thorium Data Manual* similar to the chapter on thorium in the *Reactor Handbook* has been

issued in the United Kingdom.[30] The manual includes sections on the physical properties, mechanical properties, chemical properties, and thermal-cycling and irradiation properties of thorium.

Ames[31] reports that four compounds exist in the thorium-zinc system. A eutectic was found at 11 wt.% zinc and 1040°C between thorium and the first compound, $Th_2Zn$, which melts at 1053°C. Eutectics occur also at 21 wt.% zinc and 945°C, at 45 wt.% zinc and 1045°C, and at 65 wt.% zinc and 955°C between the compounds $ThZn_2$, which melts at 1105°C, $ThZn_4$, which melts at 1095°C, and $Th_2Zn_{17}$, which melts at 1015°C. A eutectic exists at 419°C between $Th_2Zn_{17}$ and zinc at nearly 100 wt.% zinc.

Thermal analyses[31] suggest that the thorium-yttrium system is a eutectic system, with the eutectic at about 1385°C and 30 wt.% yttrium. Metallography also indicates a eutectic at 30 wt.% yttrium. Other studies suggest liquid immiscibility in the thorium-magnesium system at compositions containing less magnesium than $ThMg_5$. The eutectic in the thorium-tantalum system is at 1565°C rather than at 1700°C as previously reported.

The magnetic susceptibility of crystal-bar thorium is reported[31] to be $0.410 \pm 0.002$ emu/g in the temperature range from 136 to 300°K. Small amounts of hydrogen were found to have relatively little effect on the strength and ductility of thorium, but large amounts decrease both of these properties.

Studies at Atomics International[32] suggest that it is impractical and probably not worth the trouble to attempt to coarsen the size of the uranium particles in thorium-uranium alloys. Data are presented which show that it takes over a year at 800°C to change the precipitate from particles which are unresolvable at 1000-diameter magnification to particles which can be resolved as metal spheres in the thorium. The effect of higher temperatures was not investigated.

British workers[33] have completed an investigation of the hot hardness and metallography of some thorium-rich alloys. Thorium-aluminum alloys show precipitation-hardening effects; thorium-uranium alloys show no increase in hot hardness up to 800°C with uranium additions up to 3 at.%; and thorium-zirconium alloys show increased hardness at temperatures up to 800°C for compositions up to the solubility limit of zirconium in thorium. Aluminum and uranium in excess of their solubility limits in thorium restrict grain growth at temperatures as high as 1150 and 1200°C.

G. A. Meerson and A. F. Islankima[34] of the U.S.S.R. have compared the properties of pressed and sintered thorium powders produced by electrolysis and by calcium reduction. Powders of both types were cold pressed and sintered at 1200 to 1400°C. The properties of the products are shown in the following tabulation:

| | Electrolytic compacts | Calcium-reduced compacts |
|---|---|---|
| Density, g/cm³ | 11.6 | 11.5 |
| Brinell hardness, kg/mm² | 50 | 70 |
| Ultimate tensile strength, psi | 23,500 | 31,000 |
| Elongation, % | 35–43 | 17–23 |

These results show that the electrolytic thorium used in these studies is similar in quality to iodide thorium.

Densities of iodide-thorium-base thorium-uranium alloys have been reported by Battelle[35] to be as follows:

| Alloy, wt.% | Density, g/cm³ |
|---|---|
| Th–5 U | 11.88 |
| Th–10 U | 12.10 |
| Th–15 U | 12.33 |
| Th–20 U | 12.58 |

In addition, Battelle reports that an X-ray examination detected both alpha and beta thorium in samples of a thorium–25 wt.% zirconium–25 wt.% uranium alloy and a thorium–20 wt.% zirconium–20 wt.% uranium alloy quenched from 1000°C. In corrosion tests in 200°C water, these quenched alloys showed comparatively good corrosion resistance. Small quaternary additions of cerium, lanthanum, ruthenium, titanium, and yttrium were found to be harmful to the corrosion resistance in water of a thorium–10 wt.% zirconium–10 wt.% uranium alloy.

Thorium alloys with various fabrication histories and heat-treatments were compared at Nuclear Metals.[36] It was found that they are usually most resistant to corrosion by 500°F water in the as-extruded or as-fabricated con-

dition. The results of corrosion tests on bare-end samples of clad thorium alloys in the as-extruded condition are shown in the following tabulation:

| Alloy, wt.% | Weight loss in 500°F water, mg/(cm²)(hr) |
|---|---|
| Th | 148 |
| Th–2 Zr | 121 |
| Th–5 Zr | 13 |
| Th–10 Zr | 26 |
| Th–9 U–2 Zr | 102 |

Fragmentary data reported by Hanford for tensile tests of irradiated thorium specimens are as follows:

| Burn-up, at.% | Yield strength, psi | Elongation, % |
|---|---|---|
| 0 | 15,500 | 42 |
| 0.08 | 50,000 | 33 |
| 0.1 | 50,000 | 13 |
| 1.0* | | 0.2 |
| 1.6 | 69,000 | 7 |

*Failed outside gauge length at oxidized cracks.

It is not clear whether the burn-up is in terms of fission of $U^{233}$ or in terms of depletion of $Th^{232}$, but the very high burn-ups and the tensile properties obtained suggest that the exposure was a very long one, presumably near room temperature. An elongation of 7 per cent after a burn-up of 1.6 at.% attests to the remarkable radiation-damage resistance of metallic thorium. (W. Chubb)

## *Refractory Fuel and Fertile Materials*

### Properties and Behavior of Uranium Oxides

Sylvania is continuing the study of the effects of additives on the thermal conductivity of $UO_2$. The thermal conductivity of sintered $UO_2$ bodies at 1200°C has been increased 30 per cent by the addition of 1 mole % yttrium oxide.[27] An interim summary of this work has recently been published.[37]

In a study of the compatibility of $UO_2$ in flowing $CO_2$, the British found[38] that bodies sintered in argon or hydrogen and tested at high temperature in dry and wet $CO_2$ for 100 to 250 hr give $U_3O_8$ as the chief reaction product. The rate of attack levels off after 40 hr. Moist gas produces a slightly higher rate of attack at all temperatures than does dry gas. An induction period, observed for bodies sintered in argon, was not observed with bodies sintered in hydrogen. Rates of attack vary from $5 \times 10^{-3}$ to $2 \times 10^{-2}$ mg/(cm²)(hr) and depend on the method of $UO_2$ preparation and $UO_2$ stoichiometry. The rate of attack for one specimen, $UO_{2.19}$, was $5 \times 10^{-3}$ mg/(cm²)(hr) in dry $CO_2$ at 900°C.

Battelle is continuing the study of $UO_2$ stabilization by valence compensation.[39] When CaO is substituted for some of the $La_2O_3$ in $UO_2$-$La_2O_3$ compacted bodies, the high-temperature stability (5 to 20 hr in 3000°F air) is poorer than that for $UO_2$-$La_2O_3$ bodies.[26] In a separate study[40] the high-temperature, high-pressure reactions of $UO_2$ are being investigated to determine the feasibility of producing new high-temperature materials. In the initial work, reactions between $UO_2$ and other oxides, normally unreactive, are being studied at pressures up to 40,000 atm and temperatures to 1000°C. Preliminary work with $U_3O_8$ has revealed a new high-pressure, high-temperature phase.

Hanford is working on a new fuel element based on the simultaneous compacting of $UO_2$ and forming of extruded aluminum-alloy cladding. Two concentric tubes, separated by equally spaced radial ribs, are filled with 40 per cent dense $UO_2$ powder and closed with welded end plugs. First, 1000-psi gas pressure is applied to this assembly, and then the assembly is isostatically (hydraulically) pressed to 50,000 psi. The final $UO_2$ density is 7 g/cm³. Such an element was irradiated to $1.3 \times 10^{20}$ nvt in the MTR at a maximum heat flux of 300,000 Btu/(hr)(ft²) and gave satisfactory performance. Internal core temperatures of 1400°C caused sintering, which resulted in shrinkage cavities. No evidence of a $UO_2$-cladding reaction was observed.

A number of survey and review papers dealing with $UO_2$ have become available recently. Runnalls[41,42] has reviewed Canadian thought on $UO_2$ fuel. An up-to-date bibliography of literature references on $UO_2$ has been compiled.[43] Preparation and characterization of $UO_2$ powders is discussed by Bettis workers.[44]

(W. S. Diethorn)

## Fabrication of $UO_2$-containing Ceramics

The Babcock & Wilcox Company[45] has been developing a rotary swaging process for the fabrication of $UO_2$ fuel elements contained in stainless-steel tubing. Nearly 10,000 ½-in.-diameter 6-ft-long rods were fabricated for critical experiments supporting the design of the power plant for the NS *Savannah*. Density of the oxide was consistently in excess of 9.3 g/cm$^3$. It was reported that process and material efficiency was in excess of 95 per cent and that all elements were performing satisfactorily after 1 year of service. (H. D. Sheets)

## Properties of Refractory Fuels Other Than Uranium Oxides

The carbides of uranium are being evaluated for use as high-temperature nuclear fuels. The methods of preparation by hot pressing and the metallography of UC and $UC_2$ have been published[46] along with corresponding data for other high-melting-point carbides. The thermal conductivity and expansion of UC are reviewed in a North American report.[47] Harwell[38] found the reaction rate of UC with $CO_2$ at 500°C to be considerably greater than that of uranium. At 700 to 1000°C the rates were similar. Battelle[23] has recently investigated the effect of impurities on the physical properties of UC. Specimens containing 5.0 wt.% carbon are somewhat weaker than those containing 4.8 wt.% carbon. Impurities of iron, silicon, tungsten, nitrogen, and oxygen in less than 800-ppm quantities have a deleterious effect upon the strength of UC. Interdiffusion rates in the UC-$UC_2$ system were found by Battelle[23] studies to be very rapid at 1980°C ($D = 2 \times 10^{-6}$ cm$^2$/sec) and appreciable at 1600°C ($D = 4 \times 10^{-8}$ cm$^2$/sec). Radiation effects upon the physical dimensions and density of UC are given in Table I-2, along with fission-gas-release data.

The method of preparation and structural data for UN are given by Kempter, McGuire, and Nadler.[48] The UN has the NaCl type structure with $a = 4.8899$ A. The theoretical (X-ray) den-

Table I-2 IRRADIATION DATA ON UC SPECIMENS*

| | Capsule BMI-23-1 | | Capsule BMI-23-2 | |
|---|---|---|---|---|
| | Specimen A1-3 (top) | Specimen A1-3 (bottom) | Specimen A1-26 (top) | Specimen A1-37 (bottom) |
| Dimensions: | | | | |
| Preirradiation, in. | 0.3746 | 0.3746 | 0.3732 | 0.3737 |
| Postirradiation, in. | 0.3760 | 0.3757 | 0.3769 | 0.3733 |
| Change, % | 0.4 | 0.3 | 0.9 | 0.9 |
| Densities: | | | | |
| Preirradiation, g/cm$^3$ | 13.368 | 13.383 | 13.3439 | 13.428 |
| Postirradiation, g/cm$^3$ | 13.27 and 13.25† | 13.0452 | 13.26 and 13.09† | 13.19 and 13.18† |
| Change, % | 0.7 and 0.9† | 2.5 | 0.6 and 2.0† | 2.5 and 2.5† |
| Temperatures: | | | | |
| Surface minimum, °F | 640 | 520 | 625 | 510 |
| Core minimum, °F | 1100 | 700 | 920 | 710 |
| Surface maximum, °F | 900 | 660 | 1075 | 895 |
| Core maximum, °F | 1600 | 1100 | 1830 | 1475 |
| Surface mean, °F | 770 | 540 | 916 | 701 |
| Core mean, °F | 1330 | | 1376 | |
| Burn-up of uranium: | | | | |
| Estimated | 0.196,‡ 1420§ | 0.213,‡ 1590§ | 0.625,‡ 4600§ | 0.765,‡ 5700§ |
| Dosimetry | 0.156,‡ 1160§ | 0.195,‡ 1460§ | 0.625,‡ 4600§ | 0.850,‡ 6400§ |
| Fission-gas release ($Kr^{85}$): | | | | |
| Estimated total produced, cm$^3$ | $5.9 \times 10^{-2}$ | | $20.9 \times 10^{2}$ | |
| Estimated released by recoil, cm$^3$ | $2.5 \times 10^{-5}$ | | $8.8 \times 10^{-5}$ | |
| Actual released, cm$^3$ | $2.4 \times 10^{-5}$ | | $9.7$ and $24.0 \times 10^{-5}$ | |

*Data are taken from reference 23.
†Two pieces of specimen were checked.
‡At.%.
§Mwd/ton.

sity for this material is 14.315 g/cm$^3$, which is somewhat greater than that of UC.

Knolls[49] has investigated the preparation, thermal stability, melting points, and high-temperature reactions with air and helium of alkali and alkaline uranates. Table I-3 gives the results of this work.

Table I-3 MELTING POINT AND STABILITY OF ALKALINE URANATES*

| Compound | Melting point, °C | Heated 24 hr | | Remarks |
|---|---|---|---|---|
| | | Temp., °C | Atmosphere | |
| $Li_2UO_4$ | 1365 | 1200 | Air | No phase change |
| $Na_2UO_4$ | 1635 | 1380 | Air | No phase change |
| $K_2UO_4$ | 1620 | 1380 | Air | No phase change |
| $MgUO_4$ | 1800 | 1380 | Air | Structure changed |
| $MgUO_4$ | 1800 | 1800 | Air | Two phase |
| $MgUO_4$ | 1800 | 1700 | Helium | Decomposed |
| $CaUO_4$ | 1800 | 1380 | Air | No change |
| $CaUO_4$ | 1800 | 1800 | Air | No change |
| $CaUO_4$ | 1800 | 1700 | Helium | Decomposed |
| $SrUO_4$ | 1800 | 1380 | Air | No change |
| $SrUO_4$ | 1800 | 1800 | Air | Two phase |
| $SrUO_4$ | 1800 | 1700 | Helium | Decomposed |
| $BaUO_4$ | 1460 | 1380 | Air | No change |

*Data are taken from reference 49.

The $ThO_2$-$SiO_2$ system was investigated[50] by solid-state reaction methods. X-ray diffraction examination of the reacted mixtures showed that only a monoclinic modification of $ThSiO_4$ could be prepared by this method. Synthesis of thorite, the natural (tetragonal) form of $ThSiO_4$, was prepared by hydrothermal means. The monoclinic modification was found to dissociate at 1975°C into $ThO_2$ and glass. (D. A. Vaughan)

### Fabrication of Ceramic Fuels

#### Other Than Uranium Oxides

The arc-melting and casting technique previously developed at Battelle for fabricating UC specimens was modified to permit the fabrication of a quantity of specimens larger than those made previously. In the modified procedure, cylindrical specimens are cast in slightly oversize graphite thimbles to give a cast diameter of 0.645 in. and a length of 2⅜ in. The specimens then are ground to the desired diameter.[35] The program on the fabrication of UC has been expanded to include sintering of UC powders made by methods other than arc melting.[26] (M. J. Snyder)

## *Mechanism of Corrosion of Fuel Alloys*

Uranium-ignition studies at Argonne[51] have been extended to include reactions in air as well as in oxygen. Unalloyed uranium and binary alloys containing 1 at.% aluminum or copper were employed in the experiments. Results have indicated that, during the burning of uranium and its alloys in air, the sample undergoes temperature cycling above the ignition temperature. In oxygen, the sample temperature rises to a high value and appears to remain constant until the sample is consumed. A lower burning temperature was observed in air. Experiments with helium-oxygen and nitrogen-oxygen mixtures have shown that a decreasing oxygen content is responsible for the lower burning temperatures. No differences in oxidation behavior were noted (1) between the unalloyed and alloyed uranium, (2) from increased gas-flow rates, or (3) from the mass of metal consumed.

Experiments on the propagation rate of burning foils have indicated an inverse relation with sample thickness. Two separate "fronts" have been observed on samples burning in air: an oxidation front and an ignition front. Only the ignition front is visible during burning in oxygen. The latter is attributed to the higher speed of propagation and the increased light emission from the burning sample. (W. E. Berry)

## *Basic Studies of Radiation Effects in Fuel Materials*

### Metallic Fuels

Two recent papers from Knolls[52] review and discuss various aspects of irradiation damage in fuels. Included are the following topics: the volume stability of fuel materials, the mechanical behavior of fuel materials during reactor irradiation, irradiation performance of highly enriched fuel, and the effects of transients and longer time anneals on irradiated uranium-zirconium alloys.

A Russian paper[53] reviews the theory of reversion in uranium–9 wt.% molybdenum. Based upon homogenization of a transformed or two-phase alloy and upon resistivity changes in a homogeneous gamma-phase alloy, the volume and radius of the thermal spike associated with a fission product are reported. The results

agree closely, the thermal-spike sphere radius being $1.8 \times 10^{-6}$ and $2.5 \times 10^{-6}$ cm, respectively, for experiments on the two-phase and homogeneous samples.

At Hanford[54] swelling has been induced in uranium by electrical-glow-discharge impregnation of xenon at elevated temperatures. A specimen exposed 48 hr at 700°C showed a 3.3 per cent increase in volume of the uranium. These developments will facilitate further fundamental studies of rare-gas behavior in uranium. Other effort[16] is in progress to measure the thickness of irradiated fuels during application of pressures up to 2000 psi at room temperature after irradiation. These experiments are expected to show whether swelling occurs in uranium-niobium by plastic deformation as a result of gas pressure or by addition of vacancies to the bubble.

A Russian paper[53] reviews work on stress relaxation during irradiation and thermal cycling and reports that the relaxation of elastic active and residual stresses resulting from neutron irradiation is very intensive in uranium and some of its alloys. Thermal cycling at 25 to 325°C also accelerates relaxation. The effects of low-temperature cycles, between −180 and 220°C and between −180 and 450°C, upon cold-worked uranium are also studied by X-ray diffraction techniques. The effects of irradiation upon the width and position of lines in X-ray diffraction patterns of uranium are reported.

Based upon theoretical considerations of internal stresses resulting from anisotropic physical characteristics, it is predicted in a 1955 paper,[55] recently released, that neutron irradiation and thermal cycling will each, under certain circumstances, reduce the creep strength of alpha uranium. This is expected, especially at low strain rates, and it is believed the effect may be large if special conditions occur.

At Hanford[28] the threshold of detectable neutron damage to uranium is being determined through a series of low-temperature, short-exposure irradiations. Specimens exposed to $10^{15}$ to $10^{18}$ nvt to produce $5 \times 10^{-7}$ to $5 \times 10^{-4}$ total at.% burn-up have been studied. In general, recovery of the yield strength, during annealing after irradiation, precedes recovery of the hardness for all exposures. At 300°C an increase in yield strength, over that expected, occurred for all exposures and is attributed to aging. Hardness data also indicate aging for the two higher exposures (2.38 and $6.65 \times 10^{17}$ nvt) after annealing treatments at 400°C. For the highest exposure ($6.65 \times 10^{17}$ nvt), practically no change occurred in the tensile strength or ductility with 25-hr anneals at 300 and 400°C. Recovery in both hardness and yield strength at 400°C was almost complete. For the lowest exposure, $2.9 \times 10^{15}$ nvt, room-temperature annealing for 1 month effected complete recovery in yield strength with practically no change in hardness. The data suggest that the occurrence of twinning, which is the primary mode of uranium deformation at room temperature, is highly dependent upon the dispersion and size of point-defect clusters. Also, foreign atoms appear to restrict the increase in twin size to a greater extent than point-defect clusters. The agglomeration of lattice defects in uranium, especially by trapping big foreign atoms, may account for the aging effects observed.

The determination of mechanical properties of uranium irradiated to 0.018 to 0.10 at.% burn-up is also under way at Hanford.[56] The effects of annealing upon the properties are also being studied. (F. A. Rough)

## Nonmetallic Fuels

A review[57] has been made of work published on the crystalline structure of irradiated surfaces. Based upon the review, increased emphasis upon ion-emission microscopy and selective etching techniques is suggested in research in this field.

Two studies of structural physics of compounds are reported. In one,[58] nuclear magnetic resonance is being developed as a means of detecting quantitatively the amount of damage and behavior of displaced ions in various compounds and materials. In the other,[59] electron-spin paramagnetic resonance of compounds is being studied. In this study, lithium monofluoride crystals have been subjected to neutron irradiations of $7 \times 10^{13}$ to $3 \times 10^{17}$ nvt. The *F* type center has been observed in all samples and apparently does not arise from impurities. Crystals subjected to X-ray radiation yield the same spectrum. *V* type centers have also been observed in crystals at room temperature after exposure to greater than $10^{15}$ nvt. Crystals receiving dosages of $10^{18}$ to $10^{19}$ nvt also exhibit resonance arising from conduction electrons in lithium metal formed by the irradiation. Other crystals and minerals are also being studied.

At Bettis[60,61] a study of neutron damage to fluorides and various oxides is in progress. Calcium fluoride, $CaF_2$ – 20 wt.% $SrF_2$, and $Al_2O_3$ are being studied[76] to determine the effects of 2, 5, and $16 \times 10^{18}$ nvt thermal exposures on the lattice parameters and line broadening. This research is part of a basic study of fission-fragment damage in ceramics.

Small amounts of irradiation, about 10 nvt, were observed[61] to destroy the structure of $U_3O_8$ depleted in $U^{235}$ content. An annealing treatment of 1 hr at 170°C was insufficient to restore the $U_3O_8$ to the crystalline form. Monoclinic $ZrO_2$ irradiated to $1.6 \times 10^{19}$ nvt was judged, based upon lattice parameters, to have changed 40 per cent of the way toward the structure of stabilized $ZrO_2$.

A number of excellent studies are reported by Chalk River,[62,63] including diffusion of xenon from irradiated $UO_2$, analysis of reentry of fission gases due to fission-product collision and recoil, and analysis of a series of short-time irradiations of $UO_2$, giving interpretations of microstructural changes and effects of varying diametral clearances.

The study at Chalk River[62] of the diffusion of xenon from $UO_2$ has been made on specimens after irradiation by heating in a furnace. Diffusion constants were calculated. With fused $UO_2$, the fraction evolved at any temperature was directly proportional to the square root of the time of heating and to the reciprocal of the radius of the crystals. This behavior is that anticipated from the simplest diffusion model. In contrast with specimens of sintered $UO_2$, the fraction evolved was independent of the dimensions of the $UO_2$ fragments. Apparently, diffusion from the $UO_2$ to an interior surface is the rate-controlling step, the second step being rapid permeation through the pore structure of the oxide. The diffusion coefficient was found to vary greatly among sintered pellets prepared by different techniques.

Separate appearances of melted regions and regions of grain growth in the solid state have been observed at Chalk River[63] in sintered $UO_2$ pellets irradiated for as little as 1 min. The appearance of grain growth provides a useful temperature marker if preirradiation conditions are taken into account. It appears that varying the cold diametral clearance between pellets and sheath from 0.003 to 0.014 in. has little effect on the fuel temperature for the conditions studied, and there was no effect of irradiation on the thermal conductivity for neutron exposures of $2 \times 10^{15}$ to $8 \times 10^{16}$ neutrons/cm$^2$.

At Hanford[56] the electron-transmission microstructure and diffraction patterns of thin evaporated films are being studied. During irradiation, regions of high electron scattering or absorption are formed.

Small voids have been observed at Hanford in fractured surfaces of a number of specimens of $UO_2$ irradiated to rather low burn-ups at low temperatures. As an example, small voids have been observed along the grain boundaries of sintered $UO_2$ irradiated to 0.015 at.% burn-up at about 100°C. These voids were observed in a band 300 $\mu$ wide around the periphery of the specimen, but they were not observed in a similar specimen having a burn-up of 0.05 at.%. Additional observations are mentioned in another report,[64] but a clear picture of this phenomenon has not yet emerged. (F. A. Rough)

## *References*


1. M. H. Mueller and H. W. Knott, Preferred Orientation in Rolled and in Recrystallized High-purity Uranium Rod, ANL-5887, April 1959. (Unclassified AEC report.)
2. W. R. Yario and L. T. Lloyd, Recrystallization of Heavily Cold-rolled Uranium Sheet, ANL-5966, May 1959. (Unclassified AEC report.)
3. Q. C. Carloni and L. Lewis, Effect of Transfer Time on the Recrystallization Behavior of Beta-cooled Uranium, BRB-46, Jan. 12, 1959. (Unclassified AEC report.)
4. J. H. Kittel, Preliminary Experiments on Irradiation Cycling and Partial Beta-phase Irradiation of Uranium, ANL-5712, April 1959. (Unclassified AEC report.)
5. B. R. Butcher, The Deformation of Alpha Uranium at 450°C and 500°C, AERE-R-2898, April 1959. (Unclassified British report.)
6. B. E. Hopkinson, Kinetics of the Uranium-Steam Reaction, *Journal of the Electrochemical Society*, 106: 102-106 (February 1959).
7. S. J. Rothman and E. S. Fisher, A Note on the Elastic Constants of Uranium, *Nuclear Science and Engineering*, 5: 195-196 (March 1959).
8. S. N. Chatterjee, On the Structure of Uranium in Thin Film, *Acta Crystallographica*, 11: 679 (1958).
9. L. Grainger, "Uranium and Thorium," George Newnes, Ltd., London, 1958.
10. J. J. Katz and E. Rabinowitch, eds., Chemistry of Uranium, TID-5290 (Books 1 and 2), 1958. (Unclassified AEC report.)
11. B. Blumenthal, Constitution of Low Carbon

Uranium-Carbon Alloys, ANL-5958, Feb. 2, 1959. (Unclassified AEC report.)

12. W. H. Friske, H. E. Kline, and M. H. Binstock, Uranium Alloy Development Program for OMR, NAA-SR-3169, May 1959. (Unclassified AEC report.)
13. R. Smith, The Behavior of Hydrogen in Uranium, AERE-M/R-2799, February 1959. (Unclassified British report.)
14. J. Lehmann and H. Aubat, Grain Refining of Uranium, HW-tr-1, December 1959. (Unclassified AEC translation.)
15. A. G. Harding and M. B. Waldron, Transformations in Uranium Alloys with High Solute Solubility in the B. C. C. Gamma Phase. Part I. Preliminary Observations on the "Banded Structures" Produced by Nonequilibrium Transformations in Uranium Alloys, AERE-M/R-2673, September 1958. (Unclassified British report.)
16. Westinghouse Electric Corp., 1959. (Unpublished.)
17. P. C. L. Pfeil, J. D. Browne, and G. K. Williamson, The Uranium-Niobium Alloy System in the Solid State, *Journal of the Institute of Metals*, 87: 204-208 (February 1959).
18. R. W. Dayton and C. R. Tipton, Jr., Progress Relating to Civilian Applications During June 1959, BMI-1357, July 1, 1959. (Unclassified AEC report.)
19. R. F. Hills et al., Transformation of Metastable Phases in the Uranium-Molybdenum Alloy System, AERE-M/R-2840, March 1959. (Unclassified British report.)
20. J. E. Antill, K. A. Peakall, and M. Gardner, Oxidation of Uranium-Molybdenum Alloys in Carbon Dioxide and Air at 500–1000°C, AERE-M/R-2805, February 1959. (Unclassified British report.)
21. G. Cabane, Uranium Alloys of High Alloying Content, HW-tr-4, February 1959. (Unclassified AEC translation.)
22. A. G. Harding, M. B. Waldron, and C. Knight, Transformation in Uranium Alloys with High Solute Solubility in the B. C. C. Gamma Phase. Part II. Transformation in Uranium Alloys of 5 at.%, 10 at.%, and 20 at.% Titanium on Quenching from the Gamma Phase, AERE-M/R-2673A, December 1958. (Unclassified British report.)
23. R. W. Dayton and C. R. Tipton, Jr., Progress Relating to Civilian Applications During May 1959, BMI-1346, June 1, 1959. (Confidential AEC report.)
24. J. J. Huet, Preparation of Aluminum-Uranium Alloys by Reduction of a Uranium Salt in an Aluminum Bath, June 26, 1958, Brussels, Belgium.
25. F. J. Stubbs and C. B. Webster, The Release of Fission Product Rare Gas from a Uranium-Zirconium Alloy During Irradiation in the BEPO Reactor, AERE-C/M-372, February 1959. (Unclassified British report.)
26. R. W. Dayton and C. R. Tipton, Jr., Progress Relating to Civilian Applications During April 1959, BMI-1340, May 1, 1959. (Unclassified AEC report.)
27. J. L. Zambrow and I. Sheinhartz, in Quarterly Technical Progress Report for Period Ending March 31, 1959, SCNC-296, May 1959. (Confidential AEC report.
28. U. S. Atomic Energy Commission, May 1959. (Unpublished.)
29. U. S. Atomic Energy Commission, June 1959. (Unpublished.)
30. E. L. Francis, comp., Thorium Data Manual, IGR-R/R-303, 1958. (Unclassified British report.)
31. Semi-Annual Summary Research Report in Metallurgy, January–June 1958, ISC-1050, March 1959. (Unclassified AEC report.)
32. G. G. Bentle, Annealing Effects in Thorium-Uranium Alloys, NAA-SR-2969, June 1959. (Unclassified AEC report.)
33. R. C. Burnett and J. R. Murray, Hot Hardness Tests on Thorium and Some Thorium-rich Alloys, AERE-M/M-217, January 1959. (Unclassified British report.)
34. G. A. Meerson and A. F. Islankima, Metallic Thorium, *Atomnaya Energiya*, 5(2): 155-165 (1958).
35. R. W. Dayton and C. R. Tipton, Jr., Progress Relating to Civilian Applications During March 1959. BMI-1330, April 1959. (Unclassified AEC report.)
36. Fundamental and Applied Research and Development in Metallurgy, Progress Report for February 1959, NMI-2075, March 1959. (Secret AEC report.)
37. H. Shapiro and R. M. Powers, Uranium Dioxide Fuel Materials with Improved Thermal Conductivity, SCNC-271, June 1959. (Unclassified AEC report.)
38. J. E. Antill et al., Compatibility of $UO_2$, UC, and Uranium with $CO_2$, AERE-M/M-168, 1957. (Unclassified British report.)
39. W. B. Wilson, Stabilization of $UO_2$ by Valence Compensation, BMI-1318, Feb. 4, 1959. (Unclassified AEC report.)
40. W. B. Wilson, Application of Ultrahigh-pressure High-temperature Equipment to Study $UO_2$ Reactions, BMI-1328, Mar. 18, 1959. (Unclassified AEC report.)
41. O. J. C. Runnalls, Uranium Dioxide Fuel Elements, CRL-55 (AECL-754), Jan. 28, 1959. (Unclassified Canadian report.)
42. O. J. C. Runnalls, Economic Fuelling with Uranium Dioxide, CRL-56 (AECL-808), Apr. 8, 1959. (Unclassified Canadian report.)
43. H. H. Hausner, comp., Bibliography on Uranium Dioxide, AECU-4142, March 1959. (Unclassified AEC report.)
44. J. C. Clayton and S. Aronson, Some Preparation Methods and Physical Characteristics of $UO_2$

Powders, WAPD-178, December 1958. (Unclassified AEC report.)

45. L. R. Weissert, W. Markert, Jr., and V. J. Duplin, Jr., Fabrication of the Nuclear Merchant Ship Reactor Critical Experiment Fuel Rods by the Swaging Process, *Transactions of the American Nuclear Society*, 2(1): 128-129 (June 1959).
46. H. P. Roth, comp., Technical Papers of the Eleventh Metallographic Group Meeting Held at Bridgeport Brass Company, November 7 and 8, 1956, TID-7567(Pt. 1), Jan. 12, 1959. (Unclassified AEC report.)
47. C. A. Smith and Frank Rough, Properties of Uranium Monocarbide, NAA-SR-3625, June 1, 1959. (Unclassified AEC report.)
48. C. P. Kempter, J. C. McGuire, and M. R. Nadler, Uranium Mononitride, *Analytical Chemistry*, 31(1): 156-157 (1959).
49. J. F. White, ed., Minutes of the Uranium Dioxide Conference, Chalk River, Ontario, January 5 and 6, 1956, TID-7514, July 1956. (Unclassified AEC report.)
50. L. A. Harris, Preliminary Study of the Phase Equilibrium Diagram of $ThO_2$-$SiO_2$, *Journal of the American Ceramic Society*, 42(2): 74-77 (1959).
51. Chemical Engineering Division Summary Report for October, November, December, 1958, ANL-5959, March 1959. (Unclassified AEC report.)
52. A. H. Willis et al., Fuels, in Reactor Technology Report No. 8, KAPL-2000-5, March 1959. (Unclassified AEC report.)
53.* S. T. Konobeevsky et al., On Some Physico-Chemical Processes Occurring in Fissionable Materials Under Irradiation, A/CONF.15/P/2192.
54. J. M. Tobin and J. H. Sako, A Laboratory Apparatus for Producing Swelling in Uranium, HW-59701, Mar. 19, 1959. (Unclassified AEC report.)
55. A. M. Cottrell, Creep of Alpha Uranium During Irradiation or Thermal Cycling, AERE-M/M-102, November 1955. (Unclassified British report.)
56. F. W. Albaugh, Hanford Atomic Products Operation, Apr. 15, 1959. (Unpublished.)
57. John J. Antal, Irradiation Effects on Crystal Surfaces, MRL-39, 1958, Materials Research Laboratory, Mass.
58. P. J. Bray, Radiation Damage Studies in Solids; Nuclear Resonance Absorption Technique, NYO-7625, Dec. 1, 1958. (Unclassified AEC report.)
59. P. J. Bray and A. O. Williams, Jr., Radiation Damage Studies Using the Techniques of Electron-Spin Paramagnetic Resonance, NYO-8532, Mar. 23, 1959. (Unclassified AEC report.)
60. E. K. Halteman, in Technical Progress Report, Pressurized Water Reactor (PWR) Project for the Period December 24, 1958, to February 23, 1959, WAPD-MRP-78, March 1959. (Unclassified AEC report.)
61. B. Lustman, in Technical Progress Report, Pressurized Water Reactor (PWR) Project for the Period February 24, 1959, to April 23, 1959, WAPD-MRP-79, May 1959. (Unclassified AEC report.)
62. A. H. Booth and G. T. Rymer, Determination of the Diffusion Constant of Fission Xenon in $UO_2$ Crystals and Sintered Compacts, CRDC-720 (AECL-692), August 1958. (Unclassified Canadian report.)
63. A. S. Bain and J. A. L. Robertson, $UO_2$ Irradiations of Short Duration, CRFD-825 (AECL-806), April 1959. (Unclassified Canadian report.)
64. F. W. Albaugh, Hanford Atomic Products Operation, Jan. 15, 1959. (Unpublished.)

---

*Second United Nations International Conference on the Peaceful Uses of Atomic Energy, Geneva, September 1958. (Individual papers are available from the Office of Technical Services, Dept. of Commerce, Washington 25, D. C. Bound volumes of papers are available from United Nations, Office of Public Information, New York.)

## Graphite

Thermal-annealing studies of pitch-coke graphites irradiated at about 450°C have been carried out at Hanford.[1] Four samples which had contracted from 0.02 to 0.05 per cent during an exposure of 742 Mwd/at were annealed to a maximum temperature of 2600°C in 500°C intervals. No increase in length was caused by the heat-treatments. These data support the theory that irradiation-induced contraction in graphite results from relief of stresses frozen in during fabrication.

Studies of total stored energy content in irradiated graphite are being conducted at the Windscale Works.[2] The data in Table II-1 are of particular interest because of the temperature range covered.

Table II-1 TOTAL STORED ENERGY OF IRRADIATED GRAPHITE*

| Irradiation temp., °C | Integrated dose, neutrons/cm$^2$ | Stored energy, cal/g |
|---|---|---|
| 252 | $4.8 \times 10^{20}$ | 49 |
| 230 | $5.7 \times 10^{20}$ | 55 |
| 193 | $5.3 \times 10^{20}$ | 61 |

* Data are taken from reference 2.

Studies of constant-load tensile creep of artificial graphites at 3000 to 5300°F for periods up to 8 hr were made by the Jet Propulsion Laboratory.[3] Stresses of 1600 to 4000 psi were applied to specimens having a gauge section ¼ in. in diameter by 1 in. in length. Creep rates up to $10^{-3}$ per second were observed at the more stringent conditions. The measured creep rates increased continuously with increasing temperature. Elongations up to 40 per cent and density decreases up to 18 per cent were observed. The creep rate for given stresses and temperatures appeared to be lower when the stress was parallel to the grain direction than when it was perpendicular to the grain direction.

Sanderson and Porter[4] have completed a preliminary reactor evaluation of three types of graphite-$UO_2$ fuel elements in the form of 1.5-in.-diameter spheres containing about 5.3 g of 93.2 per cent enriched $UO_2$. The fuel-element types varied widely in fuel particle size and in degree of graphitization of the graphite. The elements were irradiated in the Battelle Research Reactor to about 1.8 per cent burn-up of the total $U^{235}$ content at surface temperatures of about 1200 to 1300°F. Postexposure hot-cell examination revealed no irradiation-induced changes in dimensions or mechanical properties that would prove detrimental to the operation of a pebble-bed reactor. The observed changes in mechanical properties indicated a tendency for the graphite to revert to a carbon structure. Dimensional shrinkage in elements containing fuel particles about 1 μ in diameter exceeded the shrinkage in elements containing fuel particles 150 μ in diameter by a factor of 4. This difference was attributed to the greater percentage of recoil fission fragments attenuated in the graphite when fuel particle size is small. (W. C. Riley)

## Beryllium Metal and Alloys

In the preceding issue (*Reactor Core Materials*, 2(3): 22 (August 1959)), a plot of third-dimensional ductility (bend deflection) against width-to-thickness ratio was presented for upset beryllium as well as for extruded and rolled material. The superior transverse ductility of upset material in the thickness direction of the sheet was attributed to the random orientation of the $(1\,1\bar{2}\,0)$ fracture planes with respect to any direction in the plane of the sheet. As in basal-plane-layered sheet, however, the basal planes lie primarily in the plane of the sheet. In a current report,[5] Nuclear Metals points out that basal-plane-layered sheet (produced by extruding and rolling) has very high elongation in the plane of the sheet but no elongation in the thickness direction. Upset sheet gains ductility in the thickness direction at the expense of ductility in the plane of the sheet. The

development of beryllium sheet with limited but finite ductility in three dimensions represents a truly significant achievement since such material can be considered for structural applications. Unfortunately, since this material is produced by upsetting, the size of sheet which can be produced is severely limited. Preliminary work indicates that upsetting, followed by compression rolling (i.e., rolling in a large number of directions), may produce essentially the same texture. If this is the case, much larger sheets can be made than is possible solely by upsetting.

Compatibility problems in the use of beryllium as a moderator or canning material in sodium-cooled thermal reactors have been investigated by the British.[6] Since beryllium will reduce sodium oxide at all temperatures, more stable oxide formers must be added to the liquid system. Free-energy data indicated that thorium and calcium might be suitable as getters in sodium systems. Thorium was found to be unsatisfactory, however, because of the tightly adherent oxide which formed on the metal, thus preventing further reaction. On the other hand, calcium, if carefully controlled, was markedly effective in reducing corrosion of the beryllium.

Ames Laboratory[7] has measured the elastic constants of beryllium from 4.2 to 300°K with a precision of 0.2 per cent, using the pulse-echo technique. Other mechanical-property data on beryllium are summarized in two Lockheed Missile System Division reports.[8,9] A memorandum surveying known information on the joining of beryllium has been issued recently by the Defense Metals Information Center at Battelle.[10] (A. J. Griest)

## *Solid Hydrides*

Recent research on hydride moderators has been divided mainly between studies on pure zirconium hydride and hydrided alloys of zirconium and of cerium. Hydriding characteristics and mechanical properties have received the most attention.

### Zirconium Hydride

Studies of zirconium hydride are continuing at Denver Research Institute.[11,12] Problems encountered in hydriding large specimens without cracking have been overcome for $N_H$ levels below 4.0 and above 5.5 by controlling the rate of hydrogen absorption. Cracking is believed to result when large hydrogen concentration gradients are present while the specimen is in the two-phase beta-plus-delta region. Tensile-property measurements at 600°C showed an increase in ultimate strength from 19,650 psi for 50 per cent delta material to 20,300 psi for 80 per cent delta hydride. Thermal conductivity of a specimen of $N_H = 3.92$ ranged from 0.029 ± 0.003 cal/(cm)(sec)(°C) at 530°C to 0.038 ± 0.004 cal/(cm)(sec)(°C) at 755°C.

A literature survey incorporating all the known properties of zirconium hydride, with information on fabrication and cladding techniques, has been prepared by General Atomic.[13] Data included were obtained from both classified and unclassified sources.

Metal Hydrides[14] has also prepared a supplement to their bibliography on the hydrides of the metals. Five hundred and ninety references, both classified and unclassified, deal with hydrogen-metal reactions and properties, fabrication, and uses of the hydrides.

Diffusion coefficients of hydrogen in beta zirconium have been determined at Battelle[15] as part of a study on thermal migration of hydrogen. Table II-2 shows the variation of the diffusion coefficients with temperature. Preliminary measurements of diffusion coefficients in the delta zirconium hydride show variations with both temperature and hydrogen concentra-

Table II-2 SUMMARY OF RESULTS FROM DETERMINATION OF DIFFUSION COEFFICIENTS FOR HYDROGEN IN BETA ZIRCONIUM*

| Temp., °C | Average hydrogen concentration, at.% | Pressures on membrane, mm Hg | | Diffusion coefficient, $10^{-6}$ cm²/sec |
|---|---|---|---|---|
| | | $P_1$ | $P_2$ | |
| 650 | 23 | 0.9 | 0.4 | 0.60 |
| 650 | 32 | 1.5 | 0.7 | 0.47 |
| 700 | 17.5 | 1.4 | 0.8 | 3.0 |
| 700 | 25.3 | 2.1 | 1.8 | 3.0 |
| 700 | 31.5 | 4.5 | 1.4 | 2.2 |
| 750 | 15.2 | 2.3 | 1.5 | 13 |
| 750 | 21.9 | 3.8 | 3.1 | 8.3 |
| 750 | 29.2 | 7.9 | 4.5 | 9.6 |
| 800 | 9.5 | 2.0 | 1.3 | 41 |
| 800 | 20.1 | 8.4 | 5.2 | 31 |
| 800 | 20.2 | 6.8 | 6.4 | 19 |
| 800 | 27.8 | 14.5 | 10.4 | 21 |
| 850 | 19.4 | 13.3 | 12.1 | 75 |
| 850 | 30.3 | 31.1 | 29.9 | 90 |

* Data are taken from reference 15.

tion.[16] At 600°C, the values varied from $8.8 \times 10^{-7}$ to $2.5 \times 10^{-4}$ cm²/sec in the concentration range 62.1 to 66.0 at.% hydrogen. At 700°C, the diffusion coefficients varied from $1.1 \times 10^{-6}$ to $2.5 \times 10^{-4}$ cm²/sec in the range 60.3 to 63.8 at.% hydrogen.

### Alloy Hydrides

Radiation damage studies on $ZrH_{1.65}$–2 wt.% uranium have been conducted by Battelle,[15] as part of a fueled-moderator program. After irradiation under hydrogen at the MTR to about 20 at.% burn-up of the uranium at peak temperatures of about 1300 and 1500°F, the specimens were found to be in very good condition and practically unchanged in density.

(H. H. Krause)

## *References*


1. F. W. Albaugh, Hanford Atomic Products Operation, Apr. 15, 1959. (Unpublished.)
2. J. C. Bell and G. B. Greenough, in Stored Energy in Pile Irradiated Graphite, TID-7565(Pt. 1), Mar. 17, 1959. (Unclassified AEC report.)
3. H. E. Martens, L. D. Jaffee, and D. D. Button, High-temperature Short-time Creep of Graphite, JPL-EP-583, Nov. 13, 1958, Jet Propulsion Laboratory, California Institute of Technology.
4. The Pebble Bed Reactor Program, Summary of First Capsule Irradiation, AECU-4055, Jan. 14, 1959. (Unclassified AEC report.)
5. F. M. Yans, Third-dimensional Ductility and Crack Propagation in Beryllium Sheet, NMI-1212, Mar. 18, 1959. (Unclassified AEC report.)
6. L. Boyne et al., Compatibility Problems in the Use of Beryllium as Moderator or Canning Material in Sodium-cooled Thermal Reactors, IGR-TN/W-1022, 1959. (Unclassified British report.)
7. J. F. Smith and C. L. Arbogast, in Semi-Annual Summary Research Report in Metallurgy for January–June 1958, ISC-1050, Mar. 1, 1959. (Unclassified AEC report.)
8. Jay F. Burcham, Tensile Properties of Brush Beryllium QMV Material at Room and Elevated Temperatures, LMSD-4009, Dec. 12, 1957, Lockheed Aircraft Corp.
9. Jay F. Burcham, Brush Beryllium QMV Material: Dynamic Modulus of Elasticity and Rupture Modulus at Room Temperature, LMSD-2423, May 23, 1958, Lockheed Aircraft Corp.
10. N. E. Weare and R. E. Monroe, Joining of Beryllium, DMIC-Memo-13, Mar. 30, 1959, Battelle Memorial Institute.
11. R. L. Beck and W. M. Mueller, Denver Research Institute, Jan. 15, 1959. (Unpublished.)
12. R. L. Beck and W. M. Mueller, Denver Research Institute, Apr. 15, 1959. (Unpublished.)
13. W. I. Thompson, R. Sharp, and M. Simnad, General Atomic Div., General Dynamics Corp., Aug. 14, 1957. (Unpublished.)
14. W. E. Bost, U. S. Atomic Energy Commission, June 1959. (Unpublished.)
15. R. W. Dayton and C. R. Tipton, Jr., Progress Relating to Civilian Applications During May 1959, BMI-1346, June 1, 1959. (Confidential AEC report.)
16. R. W. Dayton and C. R. Tipton, Jr., Progress Relating to Civilian Applications During March 1959, BMI-1330, Apr. 1, 1959. (Confidential AEC report.)

## *Boron-containing Dispersions*

A summary report has been issued by Bettis[1] on the possible use of boron-bearing materials for pressurized-water-reactor control materials. The two types of materials considered were (1) stainless-steel-enriched boron-powder dispersions contained in compartmented stainless-steel structural alloys and (2) copper–natural $B_4C$ powder dispersions clad with stainless steel. Many data obtained during the development program are reported, but the authors conclude that, because of manufacturing problems, little or no cost or performance advantage over the reference hafnium control rods could be obtained. The major difficulty, and consequently the highest cost operation encountered in the preparation of the compartmented stainless-steel–boron dispersions, was not the preparation of the dispersions (1.58 to 6 wt.% $B^{10}$) but the machining of the compartmented structural container. A high-strength container was deemed necessary since the boron–stainless-steel dispersion would contribute little or no strength after irradiation. Therefore the structural component should be strong enough to meet the normal strength requirements plus the strength needed to retain the helium released during irradiation. The container as designed consisted of a flat plate, 0.227 in. thick, in which 0.165-in.-diameter holes were to be drilled on 0.195-in. centers in a direction perpendicular to the long axis of the rod. The holes were to be up to 3.375 in. in length. Holes greater than 2 in. in length could not be drilled in stainless steel with the required dimensional tolerances. Drilling of even 2-in. holes in Stellite 25 alloy was impractical and expensive. Other shapes for the compartments were considered but were found to be impractical.

Roll bonding of copper-$B_4C$ dispersions with stainless steel was not found to be practical. Difficulty was encountered in the production of high-density copper-$B_4C$ compacts of large size, and in roll-cladding operations it was difficult to obtain a stainless-stainless bond at the temperatures required for bonding the copper-$B_4C$ dispersion.

A large-scale effort to produce burnable-poison dispersions of $B_4C$ in Zircaloy is in progress at Knolls. Previous work has shown that superior dispersions are obtained when spherical $B_4C$ is used, and consequently an evaluation of commercial spherical $B_4C$ is being conducted. In the powders tested, up to 20 per cent free carbon has been found, and particle shape has varied from roughly spherical to almost completely spherical. Free graphite is undesirable, but it seems that unless free graphite is present the $B_4C$ fractures during the cold-sizing operation. Development of a hot-sizing operation has eliminated the need for cold sizing of extruded strips. A large number of specimens are being irradiated under various conditions, and results of postirradiation anneals of some recently evaluated specimens are shown in Table III-1. It should be noted that, although the $B_4C$ is contained in the same fuel element, it is not dispersed in the same core strip as the fuel. Postirradiation corrosion testing of a 5 wt.% $B_4C$–Zircaloy-2 specimen irradiated to 90 at.% $B^{10}$ burn-up did not show any swelling after 250 hr in 650°F water, but after 500 hr both the irradiated and unirradiated specimens had swollen 2.5 and 1 mils, respectively. Considerable $B_4C$ was lost during metallographic preparation due to the attack around the particles.

An excellent short summary on boron and its compounds has been published in *Nuclear Engineering*.[2] Physical-property data for boron and boron carbide and the purity of commercially available boron and boron compounds are tabulated; the iron-boron and zirconium-boron phase diagrams are listed; properties of boron-aluminum dispersions have been compiled; bend-test data on irradiated dispersions of boron in Zircaloy and titanium are reported; and methods of fabricating these materials as well as boron-nickel cermets and self-bonded $B_4C$ and metal diborides are discussed. Most of the data have been previously discussed and reported, but the article is a concise review.

Table III-1 HELIUM RELEASE FROM KAPL 41-1 AND -2 AND 41-7 SPECIMENS DURING ANNEALING

| Specimen | Burn-up $U^{235}$, at.% | Burn-up $B^{10}$, % | Helium produced,* $cm^3$ | 450°C Helium release, % of theoretical | 500°C Helium release, % of theoretical | 550°C Helium release, % of theoretical | 550°C Core change, % Density | 550°C Core change, % Dimensions | 600°C Helium release, % of theoretical | 600°C Core change, % Density | 600°C Core change, % Dimensions | 650°C Helium release, % of theoretical | 650°C Core change, % Density | 650°C Core change, % Dimensions |
|---|---|---|---|---|---|---|---|---|---|---|---|---|---|---|
| 41-2R | | | | 0.78 in 45 hr | 0.88 in 48 hr | 1.68 in 50 hr | | | 5.87 in 168 hr | | | 1.44 in 22 hr | | |
| Poison | | 81.2 | 8.1 | | | | 0.68 | 0.88 | | 6.26 | 9.5† | | ‡ | |
| Fuel | 0.61 | | | | | | | 0.5 | | | 9.6 | | | |
| 41-1L | | | | 0.78 in 45 hr | 0.88 in 48 hr | 1.68 in 50 hr | | | 5.87 in 168 hr | | | 1.44 in 22 hr | | |
| Poison | | 83 | 8.2 | | | | 0.96 | 2.44 | | 6.69 | 9.3† | | ‡ | |
| Fuel | 0.61 | | | | | | | 0.4 | | | 11.2 | | | |
| 41-2K | | | | 0.78 in 23 hr | 0.28 in 46 hr | 1.98 in 41 hr | | | 6.13 in 147 hr | | | 1.73 in 65 hr | | |
| Poison | | 95 | 9.2 | | | | 0.1 | 0.89 | | 4.7 | 6.8† | | ‡ | 14 |
| Fuel | 0.85 | | | | | | | 0.16 | | | 7.7 | | | |
| 41-7G | | | | 1.25 in 91 hr | 1.27 in 94 hr | 3.56 in 67.5 hr | | | 6.42 in 66.5 hr | | | 6.42 in 72 hr | | |
| Poison | | 90 | 21.6 | | | | 0.95 | 3.1 | | 1.44 | 5.1 | | 2.0 | 8.2 |
| Fuel | 0.70 | | | | | | | 0.12 | | | 0.33 | | | 1.0 |

*Calculated from $B^{10}$ burn-up.

†These measurements are questionable because a flat-end micrometer was used, which is not suitable for specimens that exhibit greater fuel than poison swelling. Metallographic examination of 41-2R showed negligible poison swelling.

‡Vacuum failed, and the densities could not be determined because of oxidation.

Note: The densities are accurate to ±0.05 per cent.
Gas release is estimated precisely to ±10 per cent of release indicated.
Density and dimensional changes are presented with respect to postirradiation determinations. Dimensional changes were determined with a remotely operated micrometer.

Work on the irradiation resistance of natural $ZrB_2$ has shown that powder irradiated at 500°F to a calculated 94 at.% $B^{10}$ burn-up (12.5 at.% of total atoms) released only 4.7 per cent of theoretical helium produced. Results of annealing studies on this powder are shown in Table III-2. At the 1400°F heat-treatment, a sample of the gas released was analyzed, and, contrary to earlier experience, hydrogen was shown to be the major constituent, with helium present to the extent of 10 vol.%. Owing to the probability of gas-composition changes during the experiment, there is some question concerning the helium percentages given for each temperature; however, no uncertainty exists concerning total helium release.

Table III-2 HELIUM RELEASE FROM $ZrB_2$ DURING HEAT-TREATMENT

| Temp., °F | Treatment time, hr | Helium recovered,* % |
|---|---|---|
| 500 | 95 | 2.29 |
| 750 | 96 | 1.56 |
| 1000 | 71 | 31.39 |
| 1200 | 71 | 14.31 |
| 1400 | 8† | 18.65 |
| | | 68.20 |

*Based on total helium produced in sample from helium analyses.
†Tests halted at this point because of equipment failure.

X-ray diffraction studies on the irradiated powder were used to obtain data on lattice-constant changes and line broadening. The results are shown in Table III-3. Phases were identified by use of a Debye camera. No alpha zirconium or $ZrB_{12}$ could be detected. A faint pattern for $ZrO_2$ and very faint patterns for ZrB and ZrH plus $ZrH_2$ were reported. A strong pattern for $ZrB_2$ was shown.

Table III-3 LATTICE-CONSTANT CHANGES AND LINE BROADENING FOR $ZrB_2$

| | Lattice constant, A | | Line broadening, °2θ | | |
|---|---|---|---|---|---|
| | $a_0$ | $c_0$ | 001 | 100 | 101 |
| Starting material | 3.155 | 3.508 | * | * | * |
| Irradiated material | 3.218 | 3.491 | † | 0.36 | 0.62 |

*Line broadening taken as zero for starting materials, so far as radiation effects are concerned.
†Not measurable.

Zirconium diboride dispersions in $UO_2$–stainless-steel fuel elements are being investigated at Battelle.[3–5] Approximately 1 wt.% $ZrB_2$ is added to the core for use as a burnable poison. The studies have shown that $ZrB_2$ can be dispersed in the core without reaction or loss of boron. However, $ZrB_2$ containing large amounts of impurities or low boron content is not satisfactory. It also appears that vacuum sintering is necessary. (G. W. Cunningham)

## *References*


1. E. F. Losco and H. J. Snyder, Development of Boron-bearing Materials for Pressurized Water Reactor (PWR) Control Rods, WAPD-PWR-PMM-1806, January 1958. (Unclassified AEC report.)
2. H. C. Cowan, Boron- and Boron-containing Materials, *Nuclear Engineering*, 13(9): 11-17 (January 1959).
3. R. W. Dayton and C. R. Tipton, Jr., Progress Relating to Civilian Applications During April 1959, BMI-1340, May 1, 1959. (Unclassified AEC report.)
4. R. W. Dayton and C. R. Tipton, Jr., Progress Relating to Civilian Applications During May 1959, BMI-1346, June 1, 1959. (Confidential AEC report.)
5. R. W. Dayton and C. R. Tipton, Jr., Progress Relating to Civilian Applications During June 1959, BMI-1357, July 1, 1959. (Unclassified AEC report.)

## *Corrosion*

### Zirconium

Experiments have been conducted at Bettis[1] to study the effect of iron contamination of the surface on the hot-water and steam corrosion behavior of Zircaloy-2. The results may be summarized as follows:

1. Deleterious iron contamination can be avoided by rolling at temperatures below 1500°F. An iron content of 5 wt.% in the surface layer results in poor corrosion behavior.
2. In alloys containing a surface contamination of 2 wt.% iron, a lamellar microstructure will cause poor corrosion resistance and a spheroidal structure will show good behavior. It is possible by suitable heat-treatment to develop the desired spheroidal structure.
3. Residual strain induced by deformation, contrary to earlier beliefs, was found to have no effect on the corrosion resistance of iron-contaminated Zircaloy-2 in high-temperature water and steam.

Studies at Hanford[2] concerned with the hydriding of Zircaloy-2 in the presence of water vapor indicate that at 750°F small amounts of water vapor inhibit the hydriding reaction. However, as the temperature is varied and the protective oxide begins to dissolve in the metal, more water vapor is required to inhibit hydriding. It also would appear that, as the $ZrO_2$ film grows in thickness, it loses its protective qualities. This is based on the observation that, at both 932 and 1292°F, water-vapor pressures which were protective for short exposure periods were not for extended test times.

In studies[2] of the corrosion of Zircaloy-2 weldments, Heliarc- and electron-beam-welded specimens were exposed to 600°F water having a *p*H of 4.5. In general, the unetched coupons developed white corrosion products, whereas those etched to remove surface-contaminated metal prior to exposure evinced black films characteristic of corrosion-resistant material.

Research completed at Case[3] concerning the scaling of zirconium at elevated temperatures shows that zirconium initially scales at a relatively low rate which increases suddenly to a faster rate (breakaway). For air, breakaway does not occur at temperatures below 1832°F. On the other hand, no breakaway is observed when zirconium is exposed to pure oxygen, the scaling rate being consistently high.

The growth suffered by zirconium at scaling temperatures below 1832°F appears to be related to a deformation process. It is believed that the volume increase of the tightly adherent oxide causes forces to be transmitted to the underlying metal, resulting in deformation.

In studies at Argonne,[4] it has been demonstrated that, in an oxygen atmosphere, flow rates have little or no effect on ignition temperature of zirconium. On the other hand, ignition temperatures in air may be changed as much as 70°F by varying the flow rate.

From a consideration of the zirconium oxidation data, researchers at Argonne have postulated that, if an additive element is soluble in alpha zirconium, a prediction can be made regarding the effect it will exert on oxidation rate. In view of this they believe that it may be possible to predict the effect of additive elements on ignition temperatures. Additional research will be necessary to establish these points.

(W. K. Boyd)

### Aluminum

Since several of the new experimental aluminum alloys containing nickel, iron, and titanium exhibit corrosion rates superior to the X-8001 alloy under static conditions, Hanford[5] has extended their evaluation to flowing systems employing deionized water at 600°F. On the basis of average penetration rates, no significant differences were found between the X-8001 and the newer alloys. However, an alloy containing 0.6 wt.% nickel, 2.1 wt.% iron, and 0.1 wt.% titanium exhibited more resistance to erosion and/or corrosion than the X-8001 alloy.

(W. K. Boyd)

## Stainless Steels

As a part of the Yankee Atomic Electric[6] development program, stainless steels are being evaluated in borated water. No indication of stress-corrosion cracking has been noted for type 304 stainless-steel samples exposed at 600°F to waters containing up to 1660 ppm boron with and without *p*H adjustment to 9.6 with LiOH. Corrosion rates under these conditions ranged from 0.14 to 0.23 mg/(dm$^2$)(month).

Work at Knolls[7] has been concerned with the stress-corrosion cracking of American Iron & Steel Institute (AISI) type 410 stainless steel in high-purity water at 300°F. Data indicate that the type 410 material tempered at 650°F (Rockwell C 36 to 42) and stressed to 80,000 psi was not susceptible to cracking in hydrogen-ammoniated or hydrogen-LiOH waters. However, if oxygen was introduced into the above systems, cracking occurred with applied stresses as low as 60,000 psi. Nickel plating or shot peening the surface materially reduced susceptibility to stress cracking under the test conditions, as did tempering at 1100°F and higher. (W. K. Boyd)

## Niobium

A series of 22 binary and 9 ternary alloys made with commercial-purity (Fansteel) niobium has been corroded for 196 days in 680°F water at Battelle.[8,11] The binary alloys containing 35 and 45 at.% zirconium and a ternary alloy containing 28.2 at.% titanium – 6.1 at.% chromium were the most corrosion resistant. These data are in general agreement with the Westinghouse results. Initial results (mostly after 7 days of exposure) on alloys prepared from electron-beam-refined (Wah Chang) niobium indicate no significant difference in 680°F corrosion behavior as compared with the commercial-purity-based alloys.

General Electric[12] has recently released data on two niobium alloys, designated F-48 and F-50. Compositions, oxidation data, and strength data for these alloys are given in Table IV-1. The F-48 alloy, designed primarily for strength, has oxidation resistance about 20-fold better than that of unalloyed niobium at 2000°F. The F-50 alloy contains titanium to improve oxidation behavior and has oxidation resistance about 50-fold better than that of unalloyed niobium. (W. D. Klopp)

Table IV-1 PROPERTIES OF GENERAL ELECTRIC NIOBIUM ALLOYS*

| | Unalloyed niobium† | F-48 alloy | F-50 alloy |
|---|---|---|---|
| Composition, %: | | | |
| Tungsten | | 15 | 15 |
| Molybdenum | | 5 | 5 |
| Titanium | | | 5 |
| Zirconium | | 1 | 1 |
| Carbon | | 0.04–0.08 | 0.04–0.08 |
| Oxygen | | 0.03–0.06 | 0.03–0.06 |
| 2000°F air oxidation: | | | |
| Metal loss in 10 hr, mils/side | 59 | 7.2 | 2.4 |
| Weight gain in 10 hr, mg/cm$^2$‡ | 550 | 68 | 23 |
| 2300°F air oxidation: | | | |
| Metal loss in 10 hr, mils/side | 85 | 24 | 13 |
| Weight gain in 10 hr, mg/cm$^2$‡ | 800 | 218 | 122 |
| 2200°F mechanical properties: | | | |
| Ultimate tensile strength, psi | 14,800 | 47,000 | 35,000 |
| 100-hr rupture strength, psi | 4,000 | 17,000 | 12,000 |

* Data are taken from reference 12.

† Data on unalloyed niobium are from references 13 to 15.

‡ Weight-gain data for alloys are estimated from metal-loss data.

## Molybdenum

Coating of molybdenum with chromium by precipitation from a tin-chromium melt has been studied at MIT.[16] Coatings deposited isothermally at 1100°C from a chromium-saturated melt are adherent and nonporous to a thickness of about 1 mil. Although a coating of this type can protect molybdenum from oxidation for only short times (3 to 5 min at 1310°C), it can be used as a base for other coatings, such as argon-arc-sprayed coatings. (W. D. Klopp)

## Tantalum

The stability of coated tantalum at very high temperatures is under investigation at Armour Research Foundation.[17] Under an oxyacetylene torch (flame temperature of 5000°F), unalloyed sheet tantalum melts in 4 to 15 sec. The most protective coatings were a rare-earth-oxide mixture (termed R.E.O.) or a zirconia coating in conjunction with a copper plate behind the tantalum to act as a heat sink. $MoO_3$ is useful as an expiration coolant with R.E.O., allowing lives up to 75 sec under the oxyacetylene flame.

Under a water-stabilized plasma-arc jet (flame temperature of 20,000°F), unprotected tantalum melts in 0.5 sec. The use of a heat sink and expiration coolant is important under these conditions. A maximum life of 19 sec was obtained with R.E.O. plus $MoO_3$ plus copper backing. (W. D. Klopp)

The LAMPRE (Los Alamos Molten Plutonium Reactor Experiment) reactors now in the development stage at Los Alamos are based on the containment of selected molten-plutonium-alloy fuels by tantalum. Major emphasis in this program has been placed on exploration of the corrosion behavior of tantalum by the fuel of particular interest, a plutonium-iron alloy. Early investigations indicated that the susceptibility of tantalum to attack is directly related to the interstitial contamination present. Tantalum prepared by melting ultrapure powders with the electron-beam process has exhibited good resistance to attack in tilting-furnace exposures,[18] although there have been unexplained instances where such material has suffered considerable damage. In general, this damage occurs at grain boundaries.

A paper[19] presented at the Second International Conference on the Peaceful Uses of Atomic Energy summarizes experiments which demonstrate that:

1. Tantalum systems withstand corrosion attack well when exposed to (a) the thorium-magnesium eutectic at 800 to 900°C, (b) 95 wt.% bismuth–5 wt.% uranium at 950 to 1050°C, and (c) 90 wt.% bismuth–10 wt.% uranium at 1000 to 1100°C.
2. Yttrium is promising for containment of the uranium-chromium eutectic in the 900 to 1000°C range.

Further corrosion work along these lines is continuing. A recent report[20] describes niobium-capsule experiments with the thorium-magnesium eutectic; no appreciable attack was observed after 1000 and 1300 hr at 850°C. A dynamic loop is being constructed of yttrium for experiments with a 95 wt.% uranium–5 wt.% chromium alloy circulating at 1000°C.

Oak Ridge conducted high-temperature in-pile liquid-metal-loop experiments[21] which demonstrated that normal corrosion in lithium–type 316 stainless steel and in sodium-Inconel systems is not altered by irradiation. The single lithium-containing system was subjected to a fast-neutron dosage of $3 \times 10^{16}$ nv for 160 hr in the 1000°F range. Three sodium-containing systems were exposed to fast-neutron doses ranging from $1.8 \times 10^{16}$ to $4 \times 10^{16}$ nv; maximum and minimum system temperatures of 1500 and 1100°F were maintained during exposures lasting from 101 to 235 hr. Flow velocities in all experimental systems were in the 1 to 2 ft/sec range.

Attention is called to a volume of papers[22] presented at a recent American Society for Metals seminar on "Liquid Metals and Solidification." Of particular interest to those involved in liquid-metal corrosion problems is a treatise on solid metal–liquid metal reactions in bismuth and sodium. The status of corrosion and mass-transfer theories is presented in considerable detail. Emphasis is also placed on describing various corrosion aspects of the liquid uranium-bismuth system. (J. H. Stang)

## Iron-base Alloys

The Air Force has reported[23] the results of field tests on an iron–10 wt.% aluminum-base alloy in service at temperatures from room temperature to 2000°F. Corrosive environments tested included phosphatizing baths (near room temperature), glass baths, a neutral salt bath ($BaCl_2$-NaCl mixture), carburizing atmosphere, and a "controlled atmosphere" (probably a partially combusted gas atmosphere). Service temperatures were generally between 1000 and 2000°F.

Iron containing 10 wt.% aluminum is highly resistant to oxidation in fully oxidizing atmospheres, comparing very favorably with the 80 wt.% nickel–20 wt.% chromium type of alloy. The parts tested were corroded severely in the phosphatizing bath cycle (which included a 10 per cent $H_2SO_4$ pickling bath), in the neutral salt bath (intergranular corrosion), and by $Na_2SO_4$ additions to glass baths. However, the iron–10 wt.% aluminum alloy withstood the carburizing- and controlled-atmosphere tests very well. Environments similar to these often result in rapid intergranular corrosion of oxidation-resistant nickel-chromium alloys.

The final results of a Martin investigation of the oxidation of iron-aluminum-base alloys at 1600°F were disclosed.[24] Modifications included variations in aluminum, chromium, titanium, niobium, and zirconium additions. Alloys studied and the oxidation test results reported are shown in Table IV-2. These data show zirconium to

Table IV-2 OXIDATION OF VARIOUS IRON-ALUMINUM-BASE ALLOYS AFTER 800 HR AT 1600°F*

| Alloy composition (balance Fe), wt.% | | | | | 1600°F, 800-hr oxidation | |
|---|---|---|---|---|---|---|
| Al | Cr | Ti | Nb | Zr | Penetration, mils | Weight gain, mg/cm² |
| 5 | 5 | 0.5 | 1.0 | 0 | 0.02 | 0.04 |
| 7 | 5 | 0.5 | 1.0 | 0 | 0.07 | 0.20 |
| 11 | 5 | 0.5 | 1.0 | 0 | 0.03 | 0.00 |
| 7 | 2 | 0.5 | 1.0 | 0 | 0.04 | 0.05 |
| 7 | 11.3 | 0.5 | 1.0 | 0 | 0.06 | 0.39 |
| 7 | 5 | 0 | 0 | 0 | 0.05 | 0.05 |
| 7 | 5 | 0.5 | 0 | 0 | 0.06 | 0.04 |
| 7 | 5 | 0 | 1.0 | 0 | 0.07 | −0.84 |
| 7 | 5 | 0.5 | 0 | 0.5 | | 0.86 |
| 7 | 5 | 0.5 | 0 | 1.5 | | 1.86 |
| 7 | 5 | 0.5 | 0 | 2.5 | | 3.68 |
| 7 | 5 | 0.5 | 1.0 | 0.5 | | −0.18 |
| 7 | 5 | 0.5 | 1.0 | 1.5 | | 1.06 |
| 7 | 5 | 0.5 | 1.0 | 2.5 | | 2.19 |
| 7 | 5 | 0.5 | 2.0 | 0.5 | | −0.36 |
| 7 | 5 | 0.5 | 2.0 | 1.5 | | 0.67 |
| 7 | 5 | 0.5 | 2.0 | 2.5 | | 2.22 |

* Data are taken from reference 24.

be detrimental to the oxidation resistance of the base composition (as had been concluded previously). Variations of the other base components had relatively little effect. It was concluded that the oxidation resistance at 1600°F of most alloys studied was satisfactory and that factors other than oxidation resistance (ductility, hot strength, etc.) would determine the precise composition for use of this alloy in reactor application. (E. S. Bartlett)

## High-temperature Alloys

A program was initiated at Aerojet-General to evaluate materials for structural service in gas-cooled reactors.[25] Oxidation tests in 200-psi air at 1750°F are in progress on AISI 318, Carpenter-20 Nb, INOR-8, Hastelloy R-235, Hastelloy X, and Inco 702 and will continue to 10,000 hr. Tests for 1000 hr in 300-psi air at 1750°F are planned for Inconel and Inconel X in addition to the alloys currently under evaluation in the 10,000-hr 200-psi air test.

(E. S. Bartlett)

## Magnesium Alloys

Investigation of the corrosion behavior of magnesium alloys in 175°F $Mg(OH)_2$-inhibited water was continued at Chalk River. Alloys containing from 3.5 to 9.6 wt.% aluminum exhibited corrosion rates of about 0.5 to 1 mil/year. Magnesium–6.5 to 8.6 wt.% aluminum–1 wt.% zirconium–0.5 wt.% manganese alloys tested under stress failed by stress-corrosion cracking in 1 week. The lower aluminum modification (3 wt.%) was intact after 2 weeks of stressed exposure. Tests are continuing. No galvanic corrosion was observed after 3 weeks of exposure when magnesium was coupled with stainless steel in the test environment.

A recent French general review of knowledge[26] on corrosion of magnesium alloys reports that calcium, as well as beryllium, is very beneficial in lowering the oxidation rate of magnesium. Corrosion tests on magnesium in nitrogen at 932°F show that the metal is attacked at about one-third of the normal rate in air at that temperature. Zinc increases the rate of oxidation of magnesium at elevated temperatures because of sublimation of the zinc, which leaves crevices in the surface of the magnesium. The ignition temperatures of several magnesium alloys in different environments are presented.

(E. S. Bartlett)

## Yttrium

Recent research findings, coupled with favorable nuclear properties of the metal, have sparked interest in the use of yttrium as an addition element for certain alloys for potential use in reactor applications. The resistance of yttrium to attack by water vapor was studied in an Ames Laboratory program.[27] At temperatures between 1337 and 1472°F, the reaction occurs logarithmically, following the equation

$$W = K \log (1 + t + 0.25\,t^2)$$

The competing processes responsible for this behavior are oxidation ($Y_2O_3$) and hydride formation ($YH_2$). No free hydrogen is evolved as a result of the reaction. At a thickness of about 0.015 mm, the coating protects the underlying yttrium metal from further attack to a large degree. (E. S. Bartlett)

## Chromium

Work of Konev et al.,[28] on mechanisms and reaction rates for the oxidation of chromium in oxygen and in air showed that pure $Cr_2O_3$ is formed by the reaction of pure oxygen at $^1/_5$ atm pressure with chromium at temperatures from 1300 to 1830°F. In air at the same temperature

and oxygen partial pressure, expansion of the $Cr_2O_3$ lattice was observed, and this was attributed to the solution of nitrogen in the oxide. A layer of $Cr_2N$ was observed between the base metal and the oxide layer upon oxidation in air. It was indicated that the reaction proceeds by the inward diffusion of oxygen or oxygen and nitrogen atoms through the scales. Scaling rates in air were less than those in pure oxygen, indicating lower diffusion rates for oxygen in the nitrogen-enriched $Cr_2O_3$ lattice.

(E. S. Bartlett)

## *Zirconium-Water Reactions*

Recent results of continuing basic studies of the zirconium-water reaction have been reported by Argonne.[29] Their experiments were made on 60-mil zirconium wires which were rapidly melted and dispersed in a water-filled cell by a surge current from a bank of condensers. In the tests performed, the energy input to the wire indicated the reaction temperature, the transient pressure measured the reaction rate, the hydrogen generated gave the extent of reaction, and the particle size of residue indicated the surface area exposed to reaction.

The total extent of reaction, based on the assumption that

$$Zr + 2H_2O \rightarrow ZrO_2 + 2H_2$$

is the only reaction, is plotted in Fig. 1. It is considered likely that the scatter for the high-energy runs is due to variations in particle sizes produced by the discharge. Reaction rates were relatively low for initial temperatures below 2600°C, but it was observed that very fast, explosive pressure rises occurred for runs with an initial temperature exceeding 2600°C.

The log of the mean particle diameter is plotted as a function of reciprocal initial temperature in Fig. 2. The numbers shown represent percentage reaction. In this correlation the horizontal straight line represents the region below the melting point of zirconium. Above the melting point the extent of reaction increases (and the particle size decreases) with increasing temperature. The observed scatter undoubtedly occurs because the resulting particle size is not a unique function of temperature.

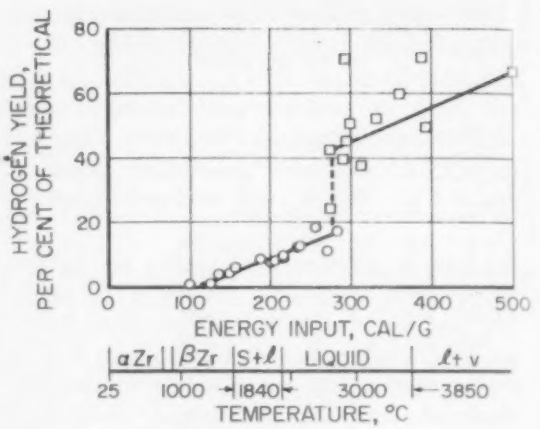


Figure 1—Zirconium-water reactions: effect of energy input on hydrogen yield. ○, slow pressure rise; □, rapid pressure rise. Data are taken from reference 29.

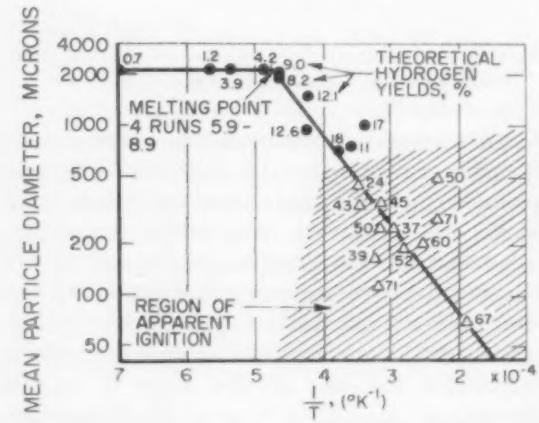


Figure 2—Zirconium-water reactions: effect of temperature on mean particle size (condenser discharge heating method). ●, slow pressure rise; Δ, explosive pressure rise. Data are taken from reference 29.

Table IV-3 TOTAL REACTION FOR PWR TYPE SIMULATED FUEL ASSEMBLIES DURING MELTING IN A STEAM ATMOSPHERE*

| Element composition | Time to melting, sec | Amount of Zr reacted, % |
|---|---|---|
| Zr-U | 45 | 7.1 |
| Zr | 60 | 3.3 |
| Zr-U | 60 | 7.0 |
| Zr-U | 230 | 8.9 |
| Zr | 300 | 19.7 |
| Zr-U | 400 | 10.0 |
| Zr-U | 430 | 11.8 |
| Zr-U | 490 | 7.1 |

* Data are taken from reference 30.

The apparent activation energy for this process is reported as 24 kcal/mole.

Mine Safety Appliances[30] conducted tests which give indications of the extent of zirconium-water reaction under simulated full-scale conditions. In their experiments Zircaloy-2-clad uranium-zirconium alloy fueled subassemblies, 15 by $2\frac{1}{2}$ by $1\frac{5}{8}$ in. and consisting of nine 70-mil-thick plates with 70-mil channels and representing a mock-up of a PWR type fuel assembly, were melted using induction heating in a steam atmosphere. Each subassembly test had a surface area of 4.28 sq ft. The characteristic mode of meltdown, the extent of chemical reaction, and the release and distribution of fission products were evaluated.

Physical damage to the subassemblies as a result of both melting and the zirconium-steam reaction was extensive with as much as 20 per cent of the material being consumed in the metal-steam reaction. Table IV-3 summarizes the results of the individual runs. Partial plugging of the channels was noted in all cases, and in one instance complete plugging of all the channels was noted. These stochastic effects are undoubtedly responsible, in part, for the lack of correlation of the reported data. It is also of interest that the release of molten metal from the subassemblies was in the form of streams rather than droplets.

(A. W. Lemmon, Jr.)

## *Radiation Effects in Nonfuel Materials*

### Basic Studies

Enhancement of short-range order configuration and a temperature-independent increase in diffuse scattering were found by measurement of diffuse X-ray scattering and peak intensities in polycrystalline copper–14.5 at.% aluminum alloy after fast-neutron irradiation.[31] These data were interpreted as resulting from static atomic displacements within localized volumes, which average out over large correlation distances. The absence of X-ray line broadening or of line shifts confirms the local nature of the damage. The results are consistent with the model[32] of metastable damage clusters of condensed vacancies and interstitials. Such clusters would cause little volume change in the surrounding matrix. Increased short-range order is pictured as a consequence of enhanced diffusion due to the radiation-produced excess of point defects.

P. Sagalyn[33] has presented calculations to demonstrate the feasibility of detecting radiation damage in a crystal lattice (particularly in metals) by nuclear magnetic resonance measurement. He estimates that in copper the atomic fraction of interstitials and vacancies needed to be detectable is about $10^{-7}$.

A Hanford report[34] has reviewed the high-temperature radiation-induced contraction of physical dimensions of graphite irradiated above 300°C. The contraction is an inverse function of degree of structure development and aeolotropy of the graphite. The contraction is apparently caused by a more efficient packing of crystallites, that is, increased density, since X-ray data show continued expansion of the $c_0$ spacing, together with a decrease of crystal size.

In a literature survey Cadoff[35] reviewed the available data on radiation-induced dimensional instability. A Harwell[36] report has reviewed the basic effects of reactor irradiation of mild steel.

(C. M. Schwartz)

### Effects of Irradiation on Mechanical Properties

Martin[24] has investigated the effects of neutron irradiation on the following three iron-aluminum-base alloys:

| | Composition, wt.% | | | | | | | |
|---|---|---|---|---|---|---|---|---|
| Alloy | Al | Cr | Ti | Zr | Cb | Mo | O | Fe |
| Fe-Al binary | 7.5 | | | | | | | Balance |
| DB-2 | 7.0 | 5.0 | 0.5 | | 1.2 | | | Balance |
| Improved Fe-Al alloy | 7.73 | 4.68 | | 1.34 | 1.20 | 2.12 | 0.032 | Balance |

The alloys were annealed and then irradiated in the MTR at doses up to $3 \times 10^{20}$ fast neutrons/cm$^2$. In general, the tensile and yield strengths increased and the elongation decreased as a result of the irradiation, as indicated in Tables IV-4 to IV-6. The annealing treatments tended to destroy the radiation damage. The irradiation failed to change the hardness, density, or dimensions significantly.

Oak Ridge has conducted two sets of tube-burst stress-rupture tests on Inconel at 1500°F

Table IV-4 EFFECTS OF IRRADIATION AND ANNEALING ON IRON-ALUMINUM BINARY ALLOY*

| Conditions of specimens | Average hardness ($R_A$) | Average strength: Yield (0.2% offset), psi | Average strength: Ultimate, psi | Average elongation, % |
|---|---|---|---|---|
| *Unannealed* | | | | |
| Unirradiated | 52.0 | 54,800 | 72,930 | 20.3 |
| Irradiated $4.57 \times 10^{19}$ neutrons/cm$^2$ | 58.4 | 83,300 | 92,450 | 12.8 |
| Irradiated $2.17 \times 10^{20}$ neutrons/cm$^2$ | 58.9 | 86,200 | 96,500 | 25.0 |
| *Annealed 3 Hr at 1600°F* | | | | |
| Unirradiated | 52.5 | 54,000 | 71,450 | 24.2 |
| Irradiated $4.57 \times 10^{19}$ neutrons/cm$^2$ | 52.3 | 60,200 | 73,000 | 28.9 |
| Irradiated $2.7 \times 10^{19}$ neutrons/cm$^2$ | 52.6 | 56,450 | 73,500 | 30.5 |

* Data are taken from reference 24.

under irradiation with the results shown in Table IV-7. The lower flux was obtained in the HB-3 facility of the MTR, and the higher, in the poolside facility of the ORR. There is good agreement of the results under both exposures. The tests show that irradiation in air at a stress of 5000 psi shortened the rupture time by at least a factor of 4. Less accurate data indicate that the rupture times are reduced at lower stresses. This effect is believed to be caused mainly by about a 0.005 per cent boron impurity in the form of $B^{10}$ transforming to helium at the grain boundaries and causing planes of weakness in the structure.

Tensile specimens of 18-8 stainless steel containing 1 per cent boron enriched to 93 per cent $B^{10}$ were fabricated by Phillips Petroleum[37] and irradiated to various amounts of burn-up. These were tested for tensile properties which are summarized in Table IV-8. There was a marked embrittlement and reduction in strength. Microexamination showed that the irradiated material was subject to pitting or etching in regions adjacent to boride inclusions in direct relation to the dose. The rapidly etching constituent probably contained lithium which formed near the boride particles and acted as a series of discontinuities in the metal to give erratic strength values.

Knolls[38] has studied the effect of irradiation on the mechanical properties of Zircaloy-3. The alloy was irradiated at 115°F under a flux up to $3.4 \times 10^{20}$ fast neutrons/cm$^2$ in the MTR. The yield strength increased by 80 per cent, the total elongation decreased by about 50 per cent, and the reduction of area remained substantially unchanged, as indicated in Table IV-9. The uniform elongation was reduced by about

Table IV-5 EFFECTS OF IRRADIATION AND ANNEALING ON DB-2 ALLOY*

| Conditions of specimens | Average hardness ($R_A$) | Average strength: Yield (0.2% offset), psi | Average strength: Ultimate, psi | Average elongation, % |
|---|---|---|---|---|
| *Unannealed* | | | | |
| Unirradiated | 58.7 | 71,000 | 100,570 | 22.1 |
| Irradiated $1.4 \times 10^{20}$ neutrons/cm$^2$ | 63.1 | 111,600 | 118,050 | 10.9 |
| Irradiated $2.0 \times 10^{20}$ neutrons/cm$^2$ | 62.1 | 105,200 | 112,250 | 17.2 |
| Irradiated $2.8 \times 10^{20}$ neutrons/cm$^2$ | 62.0 | 95,800 | 110,350 | 14.1 |
| *Annealed 3 Hr at 1600°F* | | | | |
| Unirradiated | 58.6 | 69,600 | 99,760 | 22.8 |
| Irradiated $1.4 \times 10^{20}$ neutrons/cm$^2$ | 59.2 | 70,950 | 91,750 | 5.5 |
| Irradiated $2.0 \times 10^{20}$ neutrons/cm$^2$ | 59.2 | 69,500 | 84,400 | 4.7 |
| Irradiated $2.8 \times 10^{20}$ neutrons/cm$^2$ | 59.6 | 60,200 | 93,500 | 8.7 |
| *Annealed 3 Hr at 1830°F* | | | | |
| Unirradiated | 61.5 | 70,450 | 92,250 | 23.2 |
| Irradiated $1.4 \times 10^{20}$ neutrons/cm$^2$ | 62.9 | 67,650 | 85,850 | 1.9 |
| Irradiated $2.0 \times 10^{20}$ neutrons/cm$^2$ | 63.1 | 79,000 | 101,800 | 5.5 |
| Irradiated $2.8 \times 10^{20}$ neutrons/cm$^2$ | 61.9 | 72,450 | 96,850 | 5.5 |

* Data are taken from reference 24.

Table IV-6 EFFECTS OF IRRADIATION AND ANNEALING ON IMPROVED IRON-ALUMINUM-BASE ALLOY*

| Conditions of specimens | Average hardness ($R_A$) | Average strength: Yield (0.2% offset), psi | Average strength: Ultimate, psi | Average elongation, % | Average density, g/cm³ |
|---|---|---|---|---|---|
| *Unirradiated* | | | | | |
| Unannealed | 59.5 | 76,800 | 102,400 | 15.3 | 7.097 |
| Annealed 3 hr at 800°F | 59.8 | 78,930 | 104,200 | 14.3 | |
| Annealed 3 hr at 1600°F | 60.4 | 75,000 | 101,200 | 17.9 | |
| *Irradiated 1.9 × 10²⁰ Neutrons/cm²* | | | | | |
| Unannealed | 63.1 | 108,000 | 118,500 | 16.0 | 7.088 |
| Annealed 3 hr at 800°F | 61.2 | 73,300 | 111,300 | 17.2 | |
| Annealed 3 hr at 1600°F | 60.7 | 78,600 | 103,200 | 19.2 | |

* Data are taken from reference 24.

Table IV-7 EFFECT OF NEUTRON BOMBARDMENT ON THE RUPTURE TIME OF INCONEL TUBING AT 1500°F IN AIR

| Specimen | Wall thickness, mils | Stress, psi | Flux (>1 Mev), neutrons/(cm²)(sec) × 10¹³ | Rupture time, hr |
|---|---|---|---|---|
| 71 | 30 | 3000 | 2 | 784 |
| 73 | 30 | 3000 | 2 | >869 |
| 2-2 | 30 | 3000 | 5 | 467 |
| 48 | 30 | 3000 | 0 | >2850 |
| 64 | 30 | 4000 | 2 | 343 |
| 65 | 30 | 4000 | 2 | 279 |
| 43 | 30 | 4000 | 0 | 801 |
| 44 | 30 | 4000 | 0 | 797 |
| 68 | 30 | 5000 | 2 | 94 |
| 76 | 30 | 5000 | 2 | 96 |
| 2-1 | 30 | 5000 | 5 | 91 |
| 2-5 | 30 | 5000 | 5 | 100 |
| 2-6 | 30 | 5000 | 5 | 37* |
| 35 | 50 | 5000 | 0 | 473 |
| 41 | 30 | 5000 | 0 | 487 |
| 28 | 30 | 5000 | 0 | 410† |
| 37 | 50 | 5000 | 0 | 429† |

* Low value possibly caused by 20-min temperature excursion to 1600°F.

† Tests conducted with helium inside specimen and air outside. All others had air inside and outside of specimens.

Table IV-8 EFFECT OF RADIATION ON THE MECHANICAL PROPERTIES OF $B^{10}$ STAINLESS STEEL*

| Integrated dosage, thermal nvt × 10²⁰ | Reactor | Burn-up of $B^{10}$, % | Hardness ($R_C$) | Strength, psi: Ultimate, | Strength, psi: 0.2% offset | Elongation in 1 in., % |
|---|---|---|---|---|---|---|
| 0 | | 0 | 30 | 121.9 | 93.4 | 15.6 |
| 2.6 | MTR | 15 | 37 | 153.5 | 149.5 | 3.4 |
| 4.4 | MTR | 25 | 42 | 137.1 | | 1.6 |
| 7.8 | ETR | 40 | 49 | 59.4 | | 2.5† |
| 30.5 | ETR | 90 | 51 | 24.8 | | 3.4† |

* Data are taken from reference 37.

† May be caused by growth during irradiation.

80 per cent in the longitudinal direction and 100 per cent in the transverse direction. Similar studies at Hanford[39] led to the conclusion that these effects should also be valid for Zircaloy-2 when exposed to similar (lower) flux levels.

Chalk River[40] has concluded a series of radiation-effects studies on Zircaloy-2. Tensile specimens were irradiated at 220 and 280°C with respective integrated fluxes of $3.6 \times 10^{19}$ and $2.7 \times 10^{20}$ fast neutrons/cm². The effects of the irradiation on the tensile properties and hardness are shown in Tables IV-10 and IV-11. There was an increase in proportional limit, yield strength, and ultimate tensile strength and a decrease in the total and uniform elongations. The amount of irradiation hardening increased with increasing fast-neutron flux but appeared to saturate below a flux of $2.7 \times 10^{20}$ fast neutrons/cm². The percentage changes in mechanical properties as a result of irradiation were greater in the annealed than in the cold-worked material. A yield point developed in the irradiated material tested at 280°C, whereas no yield point was present in the same material tested at room temperature. Both irradiated and control samples were annealed for 1 hr at various temperatures and then pulled at room temperature. The authors concluded that there was slight recovery occurring in all specimens during the irradiation at 280°C. Moreover, the damage could be annealed out in the region of 450°C for the material in all three conditions. The recovery curves for mechanical properties of unirradiated and irradiated cold-worked material were similar in the range 450 to 700°C and imply that recovery of cold work alone was occurring in this temperature region.

(B. C. Allen)

Table IV-9 ROOM-TEMPERATURE TENSILE TEST RESULTS ON NONIRRADIATED AND IRRADIATED ZIRCALOY-3*

| Integrated fast flux, neutrons/cm$^2$ | Capsule | MTR cycles | MTR position | Direction to rolling | Yield strength (0.2% offset), psi | Ultimate tensile strength, psi | Uniform elongation in 1.26 in., % | Total elongation in 1.26 in., % | Reduction of area, % |
|---|---|---|---|---|---|---|---|---|---|
| Preirradiated | | | | Longitudinal | 40,000 | 62,000 | 17.2 | 28.9 | 41.3 |
| Preirradiated | | | | Longitudinal | 35,300 | 61,300 | 17.4 | 28.6 | 43.3 |
| Preirradiated | | | | Longitudinal | 35,400 | 61,900 | 17.1 | 27.7 | 44.9 |
| Preirradiated | | | | Transverse | 49,700 | 59,300 | 11.3 | 30.6 | 42.0 |
| Preirradiated | | | | Transverse | 49,700 | 60,000 | 11.6 | 24.5 | 44.8 |
| $1.2 \times 10^{20}$ | 7-12-3 | 10 | L-49SW | Longitudinal | 69,700 | 73,300 | 3.6 | 20.2 | 50.6 |
| $1.2 \times 10^{20}$ | 7-12-3 | 10 | L-49SW | Longitudinal | 68,700 | 72,700 | 4.0 | 11.9 | 44.0 |
| $1.2 \times 10^{20}$ | 7-12-3 | 10 | L-49SW | Transverse | 78,300 | 78,300 | 0 | 16.5 | 52.6 |
| $1.2 \times 10^{20}$ | 7-12-3 | 10 | L-49SW | Transverse | 78,000 | 78,000 | 0 | 14.4 | 62.0 |
| $1.8 \times 10^{20}$ | 7-12-1 | 5 | L-47 | Longitudinal | 66,100 | 71,000 | 4.2 | 13.3 | 43.3 |
| $1.8 \times 10^{20}$ | 7-12-1 | 5 | L-47 | Longitudinal | 67,300 | 72,000 | 3.8 | 13.6 | 46.6 |
| $1.8 \times 10^{20}$ | 7-12-1 | 5 | L-47 | Transverse | 81,900 | 81,900 | 0 | 6.9 | 56.6 |
| $1.8 \times 10^{20}$ | 7-12-1 | 5 | L-47 | Transverse | 78,000 | 78,000 | 0 | 6.7 | 50.0 |
| $3.3 \times 10^{20}$ | 7-12-4 | 5 | L-49NW | Longitudinal | 68,000 | 72,000 | 3.5 | 16.0 | 41.3 |
| $3.3 \times 10^{20}$ | 7-12-4 | 5 | L-49NW | Longitudinal | 70,700 | 75,300 | 4.0 | 12.6 | 41.3 |
| $3.3 \times 10^{20}$ | 7-12-4 | 5 | L-49NW | Transverse | 78,000 | 78,000 | 0 | 7.6 | 51.3 |
| $3.3 \times 10^{20}$ | 7-12-4 | 5 | L-49NW | Transverse | 77,300 | 77,300 | 0 | 9.8 | 48.0 |
| $3.4 \times 10^{20}$ | 7-12-2 | 10 | L-49NW | Longitudinal | 69,300 | 72,300 | 4.1 | 17.5 | 42.0 |
| $3.4 \times 10^{20}$ | 7-12-2 | 10 | L-49NW | Longitudinal | 69,300 | 73,700 | 4.0 | 12.4 | 43.3 |
| $3.4 \times 10^{20}$ | 7-12-2 | 10 | L-49NW | Transverse | 81,500 | 81,500 | 0 | 6.0 | 42.0 |
| $3.4 \times 10^{20}$ | 7-12-2 | 10 | L-49NW | Transverse | 82,000 | 82,000 | 0 | 6.4 | 51.3 |

* Data are taken from reference 38.

Table IV-10 ROOM-TEMPERATURE TENSILE PROPERTIES OF UNIRRADIATED AND IRRADIATED ZIRCALOY-2*

| Irradiation history | Metallurgical condition | Proportional limit, 1000 psi | Yield strength (0.2% offset), 1000 psi | Ultimate tensile strength, 1000 psi | Total elongation, % | Uniform elongation, % | Proportional limit/ultimate tensile strength | Hardness ($R_B$) |
|---|---|---|---|---|---|---|---|---|
| Unirradiated | Annealed | 44.8 | 51.2 | 78.5 | 23.5 | 14 | 0.59 | 87.7 |
| Unirradiated, out of pile (280°C) | Annealed | 44.3 | 49.4 | 76.0 | 19.6 | 12 | 0.61 | |
| $3.6 \times 10^{19}$ neutrons/cm$^2$ (220°C) | Annealed | 60.9 | 65.6 | 85.1 | 19.5 | 7 | 0.72 | 89.5 |
| $2.7 \times 10^{20}$ neutrons/cm$^2$ (280°C) | Annealed | 75.7 | 79.3 | 91.4 | 12.7 | 4 | 0.83 | 91.9 |
| Unirradiated | 13.1% cold work | 84.1 | 88.1 | 92.9 | 14.0 | 3 | 0.91 | 90.1 |
| Unirradiated, out of pile (280°C) | 13.1% cold work | 70.5 | 74.5 | 84.3 | 12.3 | 4 | 0.84 | |
| $3.6 \times 10^{19}$ neutrons/cm$^2$ (220°C) | 13.1% cold work | 85.8 | 90.5 | 96.7 | 10.2 | 2 | 0.89 | 93.2 |
| $2.7 \times 10^{20}$ neutrons/cm$^2$ (280°C) | 13.1% cold work | 98.1 | 102.0 | 104.1 | 9.3 | 1 | 0.94 | 95.4 |
| Unirradiated | Tempered, 25.5% cold work | 72.6 | 77.1 | 92.5 | 15.5 | 6 | 0.79 | 91.2 |
| Unirradiated, out of pile (280°C) | Tempered, 25.5% cold work | 70.0 | 76.0 | 90.0 | 13.0 | 6 | 0.78 | |
| $3.6 \times 10^{19}$ neutrons/cm$^2$ (220°C) | Tempered, 25.5% cold work | 83.7 | 88.1 | 99.0 | 11.6 | 3 | 0.85 | 94.2 |
| $2.7 \times 10^{20}$ neutrons/cm$^2$ (280°C) | Tempered, 25.5% cold work | 95.1 | 99.4 | 105.8 | 9.4 | 3 | 0.90 | 95.3 |

* Data are taken from reference 40. Results shown are the averages of six samples tested in each condition.

Table IV-11 TENSILE PROPERTIES OF UNIRRADIATED AND IRRADIATED ZIRCALOY-2 AT 280°C*

| Irradiation history | Metallurgical condition | Proportional limit, 1000 psi | Yield strength (0.2% offset), 1000 psi | Ultimate tensile strength, 1000 psi | Total elongation, % | Uniform elongation, % | Proportional limit/ultimate tensile strength |
|---|---|---|---|---|---|---|---|
| Unirradiated | Annealed | 18.4 | 21.9 | 40.3 | 29.0 | 14 | 0.46 |
| Unirradiated, out of pile (280°C) | Annealed | 21.4 | 24.3 | 38.5 | 21.0 | 11 | 0.56 |
| $2.7 \times 10^{20}$ neutrons/cm$^2$ (280°C) | Annealed | 43.3 Y.P.† | 43.3 | 46.1 | 14.4 | 2 | 0.94 |
| Unirradiated | 13.1% cold work | 41.0 | 47.8 | 48.8 | 13.0 | 1 | 0.84 |
| Unirradiated, out of pile (280°C) | 13.1% cold work | 43.1 | 45.0 | 46.8 | 13.3 | 1 | 0.92 |
| $2.7 \times 10^{20}$ neutrons/cm$^2$ (280°C) | 13.1% cold work | 57.7 | 61.0 | 62.1 | 9 | 0.5 | 0.93 |
| Unirradiated | Tempered, 25.5% cold work | 43.9 | 47.9 | 53.1 | 12.5 | 3 | 0.83 |
| Unirradiated, out of pile (280°C) | Tempered, 25.5% cold work | 45.1 | 48.1 | 52.2 | 12.7 | 4 | 0.86 |
| $2.7 \times 10^{20}$ neutrons/cm$^2$ (280°C) | Tempered, 25.5% cold work | 58.6 | 61.7 | 62.1 | 9 | 1 | 0.94 |

* Data are taken from reference 40. Results shown are the averages of six samples tested in each condition.
† Y.P.: yield point observed in these samples.

## *Selected Metallurgical Aspects of Cladding and Structural Materials*

### Zirconium and Zirconium Alloys

Nuclear Metals[41] investigated the transformation temperatures of two zirconium-base alloys. Transformation in a zirconium–5 wt.% molybdenum–2 wt.% aluminum alloy begins at 720°C, on heating, and is complete at 800°C, and a companion zirconium–3 wt.% molybdenum–2 wt.% aluminum alloy transforms between 700 and 750°C.

Studies at Bettis[42] show that the single precipitate found in normal Zircaloy-2 is essentially a compound of zirconium and tin. Increasing the oxygen content results in an additional precipitate which is essentially a zirconium-iron compound. A zirconium-nitrogen inclusion has been found[38] and identified in Zircaloy-2 hot-rolled strip. X-ray diffraction showed the inclusion to have a face-centered-cubic structure. Its microhardness was between 882 and 933 Diamond Pyramid Hardness (DPH), and the hardness of the surrounding matrix was 192 DPH. It is probable that the inclusion has a nitrogen content between 4 and 13 wt.%.

Armour Research Foundation,[43] in studies of the zirconium-iron-tin system, has reached the conclusion that $Zr_4Sn$ and theta are distinctly different phases. Also, $Zr_4Sn$, at 24.5 wt.% tin, has negligible solubility for iron, whereas the theta phase appears at the composition 24.5 wt.% tin and 7 to 8 wt.% iron. These phases are not found in equilibrium with each other and are believed to participate in two successive four-phase ternary peritectoid reactions between 980 and 900°C in conjunction with the alpha and beta phases and $Zr_5Sn_3$; for example,

$$\text{Beta} + Zr_4Sn \rightleftharpoons \text{alpha} + Zr_5Sn_3$$

$$\text{Beta} + Zr_5Sn_3 \rightleftharpoons \text{alpha} + \theta$$

The phase $ZrFe_2$ has been firmly established at its stoichiometric composition of 55 wt.% iron. There appears to be negligible solubility for tin in this compound. Magnetic susceptibility techniques proved unsuccessful for checking the alpha + theta/alpha + theta + $ZrFe_2$ phase

boundary. However, it was found that $ZrFe_2$ has a specific magnetization of the order of 55 cgs units at room temperature and a Curie temperature of about 355°C.

In studying the tantalum-zirconium system, Ames found[44] that the monotectoid composition and temperature are at 12 wt.% tantalum and 800°C. Maximum solubility of tantalum in alpha zirconium is 1.5 ± 0.5 per cent at 800°C, decreasing rapidly with decreasing temperature. The solidus curve has a minimum near 25 wt.% tantalum and 1820°C. The curve starts to rise more rapidly at 50 wt.% tantalum to reach the melting point of tantalum at 2940°C. Below the solidus exists a continuous solid solution which decomposes on cooling except on the extreme tantalum-rich side. The intermediate alloy forms two solid solutions, and the zirconium-rich alloy transforms as a result of the beta-to-alpha transformation in zirconium, resulting in a monotectoid at 12 wt.% tantalum and 800°C. This horizontal part extends to 96 wt.% tantalum, where it is terminated by the boundary of the tantalum-rich solid solution. The solubility limit of zirconium in tantalum is about 2 wt.% at room temperature.

In the nickel-zirconium system,[44] the compound $NiZr_2$ undergoes congruent melting at 1100°C, as does NiZr at 1280°C. The $Ni_{10}Zr_7$ and $Ni_5Zr_2$ undergo peritectic decomposition at 1200 and 1180°C, respectively. The $Ni_7Zr_2$ shows congruent melting at 1420°C, and the $Ni_5Zr$ has a peritectic decomposition at 1300°C. The following crystal structures and lattice parameters were determined:

| | | |
|---|---|---|
| $Ni_5Zr$ | Face-centered-cubic | $a = 6.71$ A |
| NiZr | Orthorhombic | $a_0 \cong 3.26$ A, $b_0 \cong 9.97$ A, $c_0 \cong 4.08$ A |
| $NiZr_2$ | Tetragonal | $a_0 = 6.50$ A, $c_0 \cong 5.24$ A |
| $Ni_{10}Zr_7$ | Orthorhombic | $a_0 \cong 9.18$ A, $b_0 \cong 9.27$ A, $c_0 \cong 12.44$ A |

Eutectic points were determined at 17 wt.% nickel at 960°C, 27 wt.% nickel at 1010°C, 52 wt.% nickel at 1060°C, and 87 wt.% nickel at 1170°C. A euctectoid is located at 1.3 wt.% nickel and 840°C. The solubility of nickel in alpha zirconium is approximately 0.1 per cent at 840°C, and the maximum solubility of nickel in beta zirconium is 1.9 per cent at 960°C. Terminal solid solubility on the nickel-rich end of the diagram reaches a maximum of 3.0 wt.% zirconium at 1170°C, from which it decreases to less than 0.1 per cent zirconium at room temperature. (J. A. De Mastry)

## Niobium and Niobium Alloys

The coefficient of thermal expansion of niobium was found by Los Alamos to follow the equation:

$$\Delta_1 = 4.46 \times 10^{-3} + 1.24 \times 10^{-5}\, t + 4.836 \times 10^{-9}\, t^2$$

where $\Delta_1$ is increase in length from 25 to $t$°C for the temperature range 990 to 2332°C. The standard deviation of the fit was $7.6 \times 10^{-4}$. Some values of $\bar{\alpha}$, average linear thermal coefficient of expansion, are

| Temp., °C | $\bar{\alpha}$ ($\times 10^6$/°C) |
|---|---|
| 1000 | $8.0_8$ |
| 1400 | $8.2_6$ |
| 1600 | $8.4_6$ |
| 1800 | $8.6_9$ |
| 2000 | $8.9_3$ |
| 2200 | $9.2_0$ |
| 2400 | $9.4_9$ |

Thermal conductivity and electrical resistivity data for niobium, as determined by the British,[45] are presented in Table IV-12 and Fig. 3. (J. A. De Mastry)

## Tantalum and Tantalum Alloys

Physical properties of tantalum are being investigated by Ames.[27] Experimental data for electrical resistivity, thermal diffusivity, and the Seebeck coefficient of tantalum between room temperature and 1000°C are shown in Figs. 4 to 6. Figure 7 shows thermal conductivity curves which were calculated by two different methods, one using the theoretical Wiedemann-Franz constant and electrical resistivity data, and the second using thermal diffusivity data multiplied by the specific heat per unit volume. The agreement is remarkably good.

Ames,[44] in work on the tantalum-vanadium system, reports complete solid solubility above 1320°C. A minimum exists in the solidus at approximately 30 wt.% tantalum and 1820°C.

Table IV-12 THERMAL CONDUCTIVITY AND ELECTRICAL RESISTIVITY OF NIOBIUM

| | | | | | | | | |
|---|---|---|---|---|---|---|---|---|
| *Rectangular Specimen, Density 8.38 g/cm³* | | | | | | | | |
| Temp., °C | 0 | 100 | 200 | 300 | 400 | 500 | 600 | 650 |
| Thermal conductivity, cal/(cm)(sec)(°C) | 0.111 | 0.117 | 0.122 | 0.128 | 0.134 | 0.139 | 0.145 | 0.148 |
| Electrical resistivity, μohm-cm | 16.41 | 20.85 | 25.22 | 29.74 | 34.19 | 38.63 | 43.07 | 45.30 |
| *Cylindrical Specimen, Density 8.65 g/cm³* | | | | | | | | |
| Temp., °C | 0 | 100 | 200 | 300 | 400 | 500 | 600 | |
| Thermal conductivity, cal/(cm)(sec)(°C) | 0.125 | 0.130 | 0.135 | 0.140 | 0.145 | 0.151 | 0.156 | |
| Electrical resistivity, μohm-cm | 15.22 | 19.18 | 23.13 | 27.09 | 31.04 | 35.00 | 38.96 | |

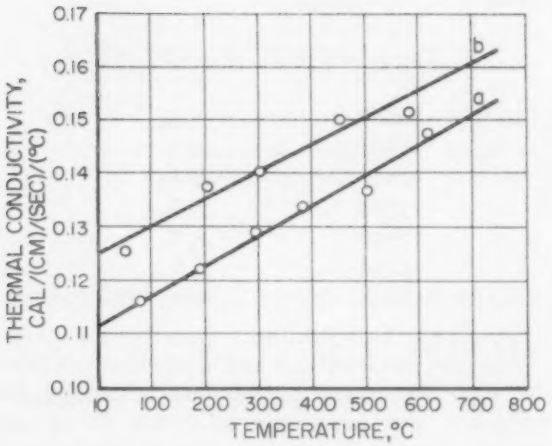


Figure 3—Thermal conductivity of niobium. a, rectangular specimen, density 8.38 g/cm³. b, cylindrical specimen, density 8.65 g/cm³. Data are taken from reference 45.

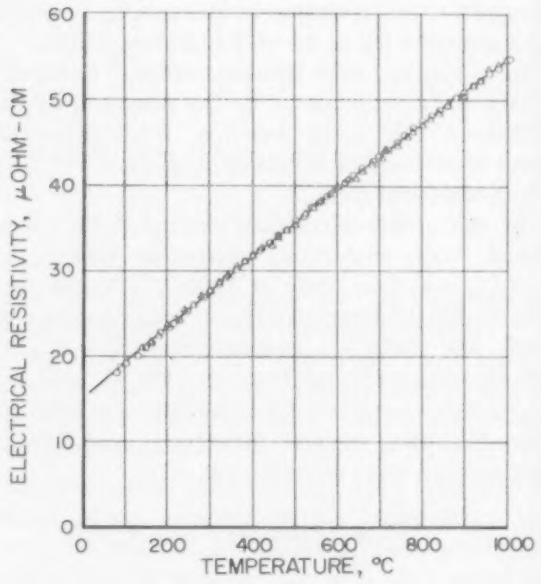


Figure 4—Electrical resistivity of tantalum. Data are taken from reference 27.

An intermediate phase, beta or $TaV_2$, is rejected from solid solution at 1320°C at approximately 64 wt.% tantalum. The beta phase has an isomorphous structure with a face-centered-cubic Laves phase, $MgCu_2$, and has a lattice parameter of $a = 8.163$ A. The boundaries of a two-phase region are from 27.5 to 87.5 wt.% tantalum at 900°C. (J. A. De Mastry)

## Aluminum and Aluminum Alloys

The existence of a ternary intermediate phase in the magnesium-aluminum-calcium system has been reported by the British.[46] This phase has a tetragonal crystal structure with an axial ratio of approximately 1.40, $c = 11.40$ A and $a = 8.12$ A. This phase exists over a narrow range of composition and may be represented by the formula $Mg_{1.3}Al_{1.7}Ca$. The axial ratio varies slightly with composition. In cast and extruded alloys with low aluminum and calcium contents, this phase and the $Mg_{17}Al_{12}$ phase may be removed by suitable heat-treatment between 400 and 500°C. (J. A. De Mastry)

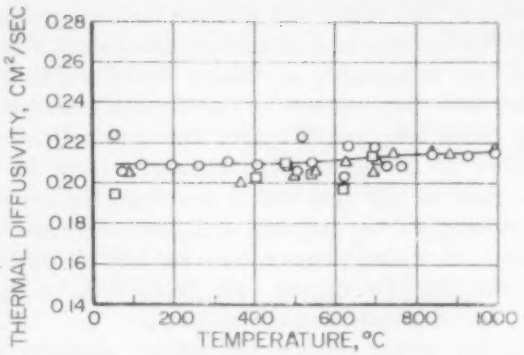


Figure 5—Thermal diffusivity of tantalum. Data are taken from reference 27.

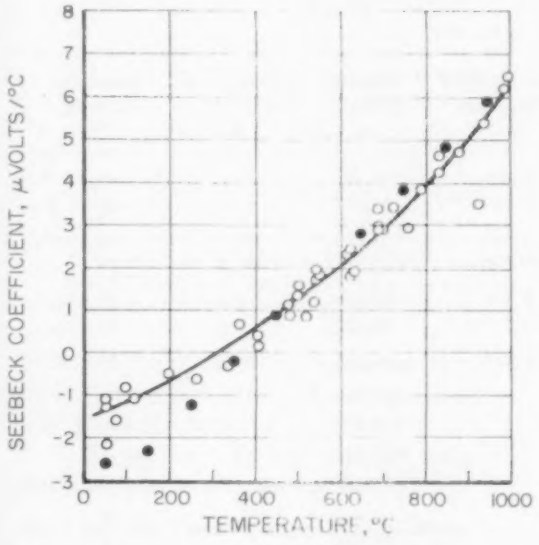


Figure 6—Seebeck coefficient of tantalum. ●, calculated from data in "Temperature, Its Measurement and Control in Science and Industry," p. 1310, Reinhold Publishing Co., New York, 1941. Data are taken from reference 27.

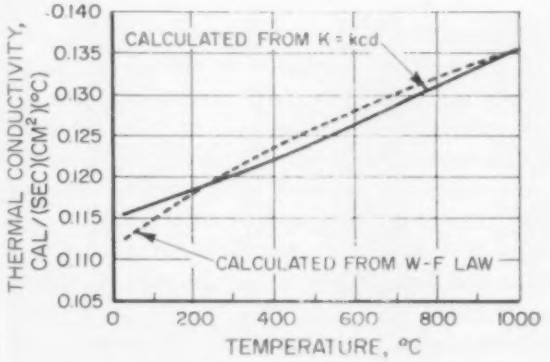


Figure 7—Thermal conductivity of tantalum. Data are taken from reference 27.

## Diffusion Studies

Diffusion in metals is reviewed by Shewon in a paper[47] which discusses alloy diffusion, diffusion in pure metals, off-diagonal terms, diffusion in liquids, diffusion of interstitials, and diffusion along surfaces. A compilation of 106 references is included in the article

A fundamental study is being made at Battelle[9] of the kinetics and mechanisms of the niobium-nitrogen reaction with emphasis on the study of diffusion and evaluation of terminal solubilities of nitrogen in niobium. Reactions carried out at 1100 and 1600°C followed a parabolic rate law with rate constants of $1.0 \times 10^2$ and $1.6 \times 10^4$ $(\mu g/cm^2)^2/sec$, respectively. At 900°C and nitrogen pressures of ¼, ½, and 1 atm, the reactions had parabolic rate constants of 0.76, 0.74, and 0.69 $(\mu g/cm^2)^2/sec$, respectively. X-ray studies on niobium samples reacted with nitrogen at 800 to 1400°C have shown that the reaction products up to and including 1000°C were both $Nb_2N$ and NbN and that those above 1000°C were cubic and hexagonal NbN. In the temperature range of 800 to 1600°C, the diffusion of nitrogen in niobium has been determined by the least-squares method to be

$$D = 0.0605 \exp(-38{,}800/RT)$$

where the activation energy is 38.8 ± 0.7 kcal/mole. From the diffusion experiments, terminal solubilities of 3.4 and 4.7 at.% nitrogen in niobium were observed at 1500 and 1600°C, respectively.

Diffusion studies of solid-liquid and solid-solid interactions between reactor materials are being carried out at Nuclear Metals.[41,48] Results of dip type experiments for the solid-liquid interaction studies have shown that zirconium and type 304 stainless-steel samples dipped into molten uranium must be cooled rapidly after dipping to prevent further reaction. A quench tube, through which helium is introduced, has been incorporated into the vacuum furnace to facilitate rapid cooling after withdrawing the samples from the liquid. For the solid-solid interaction studies, bonding experiments using special surface preparation and handling techniques have been conducted on vanadium-uranium-niobium, titanium-uranium-zirconium, and titanium-uranium-niobium diffusion couples. The improved bonding in these couples, as evidenced metallographically, shows

the importance of surface preparation, especially in regard to contamination by air and etchant products. (M. A. Gedwill, Jr.)

## *Selected Mechanical Properties of Cladding and Structural Materials*

A program to investigate the tensile, strain fatigue, and stress-rupture properties of Zircaloy-2 welds at room temperature and 600°F in the notched and unnotched conditions is in progress at Knolls. The results of notched and unnotched tensile tests performed at strain rates of 0.02 in./in./min and 18.2 in./in./min are shown in Tables IV-13 and IV-14. The hydrogen content of specimens tested was 10 to 20, 150, and 331 ppm. The only noticeable effect of increasing the hydrogen from 10 to 20 ppm to 150 ppm was to decrease the tensile strengths of the notched and unnotched specimens at room temperature but not at 600°C. Increasing the strain rate from 0.02 to 18.2 in./in./min indicated the following:

1. No effect on the unnotched ductility at room temperature and 600°F.

Table IV-13 TENSILE TEST RESULTS OF WELDED ZIRCALOY-2

(Strain Rate = 0.02 in./in./min)

| Specimen type* | Notch condition† | Hydrogen, ppm | Test temp., °F | Yield strength (0.2% offset), psi | Tensile strength, psi | Elongation in 1.1 in., % | Reduction of area, % |
|---|---|---|---|---|---|---|---|
| 1 | Smooth | 10 to 20 | Room | 56,200 | 69,400 | 17.6 | 42.4 |
| | | | | 56,500 | 71,300 | 16.5 | 36.8 |
| 1 | Smooth | 10 to 20 | 600 | 22,500 | 31,400 | 28.0 | 68.6 |
| | | | | 22,000 | 31,300 | 24.2 | 70.3 |
| 1 | Smooth | 150 | Room | 56,500 | 68,500 | 6.5 | 10.0 |
| | | | | 60,400 | 73,400 | 8.8 | 15.2 |
| 1 | Smooth | 150 | 600 | 23,500 | 31,000 | 33.0 | 71.5 |
| 1 | Notched | 10 to 20 | Room | | 106,600 | | 9.5 |
| | | | | | 110,800 | | 6.8 |
| 1 | Notched | 10 to 20 | 600 | | 52,000 | | 28.4 |
| | | | | | 47,600 | | 25.2 |
| 1 | Notched | 150 | Room | | 90,400 | | 9.5 |
| | | | | | 93,300 | | 3.8 |
| 1 | Notched | 150 | 600 | | 50,000 | | 35.2 |
| | | | | | 49,000 | | 20.7 |
| 1 | Notched | 331 | Room | | 80,500 | | 7.7 |
| | | | | | 85,000 | | 7.7 |
| 2 | Smooth | 10 to 20 | Room | 53,000 | 69,500 | 18.6 | 26.7 |
| | | | | 52,500 | 70,000 | 16.8 | 23.7 |
| 2 | Smooth | 10 to 20 | 600 | 23,700 | 34,100 | 26.7 | 72.2 |
| | | | | 23,500 | 33,800 | 19.2 | 68.6 |
| 3 | Smooth | 10 to 20 | Room | 60,000 | 73,000 | 20.3 | 40.0 |
| | | | | 60,000 | 72,800 | 17.3 | 35.0 |
| 3 | Smooth | 10 to 20 | 600 | 22,500 | 31,000 | 27.0 | 72.2 |
| | | | | 22,000 | 30,500 | 35.5 | 75.0 |
| 4 | Smooth | 10 to 20 | Room | 60,000 | 72,800 | 14.1 | 40.0 |
| | | | | 61,500 | 74,000 | 14.5 | 40.0 |
| 4 | Notched | 10 to 20 | Room | | 111,000 | | 6.8 |
| | | | | | 112,800 | | 6.8 |

* Specimen designation: 1, longitudinal, all-weld, annealed; 2, longitudinal, all-weld, as welded; 3, cross-weld, annealed; and 4, cross all-weld, annealed.

† Notch configuration: 60-deg bevel, root radii 0.003 to 0.007 in., and nominal diameter reduced from 0.160 in. unnotched to 0.113 in. at the notch.

Table IV-14 TENSILE TEST RESULTS OF WELDED ZIRCALOY-2

(Strain Rate = 18.2 in./in./min)

| Specimen type* | Notch condition† | Hydrogen, ppm | Test temp., °F | Yield strength (0.2% offset), psi | Tensile strength, psi | Elongation in 1.1 in., % | Reduction of area, % | Fracture stress, psi |
|---|---|---|---|---|---|---|---|---|
| 1 | Smooth | 10 to 20 | Room | 69,000 | 84,000 | 16.1 | 35.6 | 112,000 |
| | | | | 70,400 | 84,100 | 13.5 | 34.8 | 114,000 |
| 1 | Smooth | 10 to 20 | 600 | 20,300 | 23,800 | 26.0 | 91.0 | 77,700 |
| | | | | 20,400 | 23,500 | 20.4 | 93.0 | 124,000 |
| 1 | Smooth | 150 | Room | 67,400 | 74,900 | 3.4 | 3.3 | 77,200 |
| | | | | 67,700 | 74,800 | 3.3 | 10.6 | 83,600 |
| 1 | Smooth | 150 | 600 | 18,600 | 20,600 | 26.5 | 92.0 | 68,700 |
| | | | | 18,600 | 20,600 | 34.6 | 92.0 | 68,700 |
| 1 | Notched | 10 to 20 | Room | | 125,000 | | 4.0 | 130,000 |
| | | | | | 126,000 | | 6.9 | 135,000 |
| 1 | Notched | 10 to 20 | 600 | | 38,600 | | 81.3 | 77,000 |
| | | | | | 39,600 | | 87.2 | |
| 1 | Notched | 150 | Room | | 98,000 | | 2.0 | 99,000 |
| | | | | | 91,100 | | 2.9 | 94,000 |
| 1 | Notched | 150 | 600 | | 36,600 | | 81.7 | 63,100 |
| | | | | | 36,300 | | 86.2 | 82,200 |
| 2 | Notched | 10 to 20 | Room | | 119,000 | | 1.0 | 120,000 |
| | | | | | 115,000 | | 2.9 | 119,000 |

* Specimen designation: 1, longitudinal, all-weld, annealed; and 2, longitudinal, all-weld, as-welded.

† Notch configuration: 60-deg bevel, root radii 0.003 to 0.007 in., and nominal diameter reduced from 0.160 in. unnotched to 0.113 in. at the notch.

2. A 20 per cent increase in the room-temperature yield strength but no effect on the 600°F yield strength.

3. A 20 per cent decrease in the notched and unnotched tensile strength at 600°F.

Preliminary results from strain-fatigue tests at 600°F indicate that welded Zircaloy-2 containing 10 to 20 ppm hydrogen is not notch sensitive. Initial stress-rupture tests in the 600°F temperature range have indicated that welded Zircaloy-2 apparently exhibits strain aging similar to that observed in wrought material.

As part of a program being conducted at Bettis[1] on the effect of oxygen on the mechanical, transformation, corrosion, and fabrication characteristics of vacuum-melted Zircaloy, the hardness at room and elevated temperatures has been studied as a function of oxygen content. It was shown that oxygen up to 6330 ppm is effective in hardening Zircaloy-2 at temperatures ranging up to 500°C, but has little effect from 800 to 1000°C. There were some evidences of the existence of a thermally activated process in Zircaloy-2 in the vicinity of 400 to 500°C.

Bettis[38] has also investigated the effect of soaking time at the 600°C test temperature on the tensile properties of Zircaloy-2. It was found that soaking times up to 60 min at 600°F do not alter the mechanical properties. During this same time period, there is no increase in gaseous impurities as the result of soaking.

The creep properties of 15 per cent cold-worked Zircaloy-2 being investigated at Battelle[8] indicate that there is considerable difference in the creep strength at 345°C between annealed and cold-worked materials. An annealed specimen tested at 345°C and 25,000 psi failed in 860 hr, whereas the cold-worked material at the same temperature and stress has not failed in 12,000 hr. Battelle is also investigating the effect of a 750°C steam atmosphere on the creep properties of Zircaloy-2. For relatively short rupture times (approximately 100 hr), these creep properties have not been altered measurably by the steam atmosphere.

(F. R. Shober)

## Nickel-base Alloys

Treatments to improve the high-temperature strength properties of three nickel-base alloys

(Inconel, Hastelloy B, and INOR-8) after fabrication of sheet material have been reviewed by Oak Ridge.[49] Creep and tensile data showed, depending on the material and service condition, that improvements in strength can be obtained by any of three treatments: (1) annealing or aging, (2) carburization, and (3) environmental control during service.

Carburization produces the greatest increase in creep strength. Less pronounced improvements in the creep life are noted for nitriding and oxidizing environments over the creep life in argon. The optimum annealing or aging treatments are dependent on the anticipated service temperature and stress. These opinions are based on previously reported data for these alloys at elevated temperatures.

Investigation of thermal fatigue has been carried out at Oak Ridge.[50] The frequency range of primary interest was 0.1 to 10 cps. Subsequent internal stresses induced in the metal from the instantaneous radial temperature gradient were studied. These conditions were simulated, and results of the complex thermal stresses were studied for Inconel at 1400°F. The environment was a fused fluoride salt ($NaF$-$ZrF_4$-$UF_4$; 56-39-4 mole %), and the test conditions are given in Table IV-15.

Table IV-15 CONDITIONS OF THERMAL CYCLING OF INCONEL*

(Mean Temperature, 1405 ± 10°F; Inside Diameter of Test Section, 0.485 In.)

| Frequency, cps | Estimated inside wall temperature amplitude, °F | Wall thickness of test section, in. | Calculated pseudostress on inside wall fibers, psi | Total number of cycles |
|---|---|---|---|---|
| 0.4 | ±104 | 0.25 | 18,980 | 194,400 |
| 0.4 | ±104 | 0.415 | 21,640 | 32,000 |
| 0.4 | ±64 | 0.415 | 13,290 | 224,000 |
| 0.4 | ±64 | 0.415 | 14,330 | 508,600 |
| 0.1 | ±129 | 0.445 | 24,810 | 72,000 |
| 0.1 | ±123 | 0.445 | 23,690 | 27,000 |
| 0.1 | ±121 | 0.445 | 23,440 | 9,000 |
| 1.0 | ±63 | 0.147 | 10,500 | 360,000 |
| 1.0 | ±64 | 0.147 | 10,580 | 760,000 |
| 1.0 | ±46 | 0.147 | 7,620 | 2,200,000 |

* Data are taken from reference 50.

Metallographic examination of the inside-wall test sections was used to evaluate the extent of damage. Intergranular cracks to depths varying from 0.006 to 0.207 in. were produced at pseudostresses ranging from 7600 to 24,000 psi and exposure times ranging from 27,000 to 2,200,000 cycles. The lower stresses and lower exposure times produced less deep cracks. The heaviest and deepest cracks occurred at a frequency of 0.1 cps and a pseudostress level of 23,000 psi. The crack depth appeared to be a function of frequency with the deep cracks occurring at the lower frequencies. A plot of the pseudostress against number of cycles exhibits a characteristic fatigue type curve with a rapid decrease in the number of cycles to produce cracking as the stress level increases. (F. R. Shober)

## Stainless Steel

A summary of the mechanical and physical properties of nine commercial precipitation-hardenable stainless steels was prepared by Battelle.[51] The types of stainless steel covered in this reference are (1) martensitic (Stainless W and 17-4 PH), (2) semiaustenitic (17-7 PH, PH 15-7 Mo, AM-350 and AM-355), and (3) austenitic (A-286, 17-10P, and HNM). The more desirable characteristics of these alloys are their ease in machining, forming, and joining. The alloys can be hardened to high-strength levels by low-temperature (900 to 950°F and 1300°F) heat-treatments. They also exhibit the general corrosion and oxidation resistance of stainless steels. The austenitic type can be used at temperatures up to about 1300°F, whereas the martensitic and the semiaustenitic types are applicable to temperatures in the range of about 600 to 700°F. Room-temperature yield strengths to 180,000 psi can be obtained

in the martensitic types by simple aging at 900 to 950°F. The semiaustenitic types can be fully hardened by complex heat-treatments to room-temperature yield strengths of 175,000 to 225,000 psi. Simple aging at 1300°F of the austenitic type stainless gives room-temperature yield strengths in the range of 70,000 to 100,000 psi. These are iron-based, the major alloying elements being chromium and nickel with small additions of manganese, silicon, aluminum, molybdenum, titanium, columbium, vanadium, and phosphorus.

The Martin Company[24] has investigated iron-aluminum alloys for possible gas-cooled reactor applications because of their low thermal-neutron-capture cross sections and excellent oxidation resistance. On the basis of ductility and oxidation resistance, it was found that additions of approximately 3 per cent niobium and $\frac{3}{4}$ to $1\frac{1}{2}$ per cent zirconium to a base alloy of iron–$7\frac{1}{2}$ wt.% aluminum–5 wt.% chromium produced an improved alloy. The room-temperature properties are given, for the better alloys investigated, in Table IV-16.

Table IV-16 ROOM-TEMPERATURE TENSILE PROPERTIES OF IRON-ALUMINUM-BASE ALLOY*

| Alloy composition (balance Fe), wt.% | Condition | Yield strength (0.2% offset), psi | Ultimate tensile strength, psi | Average elongation, % |
|---|---|---|---|---|
| 7 Al–5 Cr–0.5 Ti–1.2 Nb | Unannealed | 71,000 | 100,570 | 22.1 |
| | Annealed 3 hr at 1000°F | 69,600 | 99,760 | 22.8 |
| | Annealed 3 hr at 1830°F | 70,450 | 92,250 | 23.2 |
| 7.5 aluminum | Unannealed | 54,800 | 72,930 | 20.2 |
| | Annealed 3 hr at 1600°F | 54,000 | 71,450 | 24.3 |
| 7.73 Al–4.68 Cr–1.20 Nb–1.34 Zr–2.12 Mo–0.032 C | Unannealed | 76,800 | 102,400 | 15.3 |
| | Annealed 3 hr at 800°F | 78,930 | 104,200 | 14.3 |
| | Annealed 3 hr at 1600°F | 75,000 | 101,200 | 17.9 |

* Data are taken from reference 24.

The stress-rupture life of the iron–7 wt.% aluminum–5 wt.% chromium–0.5 wt.% titanium–1.2 wt.% niobium alloy at 1650°F and 2000 psi was approximately 8 hr. Increasing the aluminum content to 13.0 wt.% decreased the stress-rupture life at 1650°F to 3.2 hr. Increasing the chromium content to 12 wt.% increased the stress-rupture life to 13.0 hr.

(F. R. Shober)

## Refractory Metals and Alloys

A summary of work on the ductile-brittle transition in refractory metals has been reported by Battelle.[52] The body-centered-cubic refractory metals, niobium, molybdenum, tungsten, and chromium, exhibit a ductile-brittle transition behavior. Data for vanadium suggest that the brittleness at low temperatures can be attributed to low-strain-rate hydrogen embrittlement. Up to now, no brittle transition has been found in tantalum.

The transition temperature is greatly influenced by testing and material conditions. The following tend to increase the temperature at which the brittle transition occurs: (1) recrystallization, (2) decreasing amounts of cold work, (3) increasing grain size, (4) increasing interstitial content, (5) increasing strain rate, and (6) introduction of triaxial stresses. Transition from ductile to brittle behavior is associated with a rapid rise in yield strength.

Other programs on niobium and niobium alloys are being pursued independently at Knolls and Bettis.

Bettis has been evaluating the room-temperature tensile properties of niobium-zirconium alloys. Two additional alloys, 67.5 wt.% niobium–32.5 wt.% zirconium and 92 wt.%

niobium–8 wt.% zirconium, have been tested. The first alloy has room-temperature properties similar to the 50-50 alloy at elevated temperatures, the 50-50 alloy being stronger at room temperature. The 92 wt.% niobium–8 wt.% zirconium alloy shows lower tensile strength (80,000 psi at room temperature) and higher ductility (approximately 60 per cent $R_A$). These properties are not reduced appreciably by increased temperatures up to 800°C (1472°F).

The room- and elevated-temperature properties of niobium–45 at.% zirconium–5.0 at.% titanium and niobium–10 at.% titanium–3 at.% molybdenum have been determined at Battelle.[8] The results are given in Table IV-17.

Table IV-17 TENSILE PROPERTIES OF NIOBIUM AND NIOBIUM ALLOYS*

| Alloy (balance Nb), at.% | Test temp., °F | Yield strength (0.2% offset), psi | Ultimate tensile strength, psi | Elongation, % |
|---|---|---|---|---|
| 45 Zr–5 Ti | 70 | 124,000 | 128,000 | 8 |
| 45 Zr–5 Ti | 600 | 87,000 | 101,000 | 6 |
| 45 Zr–5 Ti | 1200 | | 78,000 | 3 |
| 10 Ti–3 Mo | 70 | 57,000 | 67,000 | 35 |
| 10 Ti–3 Mo | 600 | 31,000 | 41,000 | 32 |
| 10 Ti–3 Mo | 1200 | 22,000 | 39,000 | 21 |

* Data are taken from reference 8.

## Other Materials

An investigation at Chalk River[53] has been completed on the study of the creep and tensile properties of magnesium alloy AZ 61 at 50°C. AZ 61 is a magnesium alloy containing approximately 6.50 wt.% aluminum–1.1 wt.% zirconium and 0.5 wt.% manganese with traces of iron, nickel, copper, silicon, and lead. The alloy specimens were tested in air in the as-extruded condition. Samples were cut transversely and longitudinally from extruded tube, as well as longitudinally from extruded rod. Creep tests were run at 50°C and several stresses between 10,000 and 35,000 psi. Extrapolation of minimum creep rates indicates that at 50°C the stress to produce a minimum creep rate of less than $1 \times 10^{-5}$ per cent per hour is 10,000 psi. In all tests, however, the minimum creep rate was based on a test time of less than 2000 hr. The transverse ultimate tensile strength of the tube at 50°C was 34,800 psi. The tensile strength decreased to 3500 psi at 400°C. (F. R. Shober)

## *References*


1. Zirconium Highlights, WAPD-ZH-17, May 1959. (Unclassified AEC report.)
2. F. W. Albaugh, Hanford Atomic Products Operation, May 1959. (Unpublished.)
3. H. B. Probst, E. B. Evans, and W. M. Baldwin, Jr., Scaling of Zirconium at Elevated Temperatures, Final Report, AECU-4113, April 1959. (Unclassified AEC report.)
4. Chemical Engineering Division Summary Report for October, November, and December 1958, ANL-5959, March 1959. (Unclassified AEC report.)
5. F. W. Albaugh, Hanford Atomic Products Operation, Apr. 15, 1959. (Unpublished.)
6. I. H. Coen and R. W. Garbe, Quarterly Progress Report for the Period April 1, 1958, to June 30, 1958, YAEC-87, July 30, 1958. (Unclassified AEC report.)
7. Henry Suss, Susceptibility of AISI 410 to Stress Corrosion Cracking in High-temperature High-purity Water, KAPL-M-HOS-6, Mar. 17, 1959. (Unclassified AEC report.)
8. R. W. Dayton and C. R. Tipton, Jr., Progress Relating to Civilian Applications During March 1959, BMI-1330, Apr. 1, 1959. (Unclassified AEC report.)
9. R. W. Dayton and C. R. Tipton, Jr., Progress Relating to Civilian Applications During April 1959, BMI-1340, May 1, 1959. (Unclassified AEC report.)
10. R. W. Dayton and C. R. Tipton, Jr., Progress Relating to Civilian Applications During May 1959, BMI-1346, June 1, 1959. (Confidential AEC report.)
11. R. W. Dayton and C. R. Tipton, Jr., Progress Relating to Civilian Applications During June 1959, BMI-1357, July 1, 1959. (Unclassified AEC report.)
12. Recent Advances in Columbium Alloys, General Electric Flight Propulsion Laboratory Department, General Electric Co. Brochure, July 1959.
13. H. Inouye, The Scaling of Columbium in Air, AIME-IMD Special Report No. 5, Jan. 31, 1957.
14. W. D. Klopp et al., Oxidation and Contamination Reactions of Niobium and Niobium Alloys, BMI-1317, Feb. 3, 1959. (Unclassified AEC report.)
15. F. R. Schwartzberg and W. D. Klopp, Elevated-temperature Mechanical Properties and Oxidation Resistance of Columbium and Its Alloys, DMIC-Memo-8, Feb. 4, 1959, Battelle Memorial Institute.

16. P. Schwarzkopf, E. B. Weglein, and J. Wulff, Chromium Coatings from Liquid Metal Solutions, December 1958, Massachusetts Institute of Technology.
17. C. A. Arenberg, Protective Coatings for Tantalum, WADC-TR-58-203, July 1958. (Unclassified USAF report.)
18. U. S. Atomic Energy Commission, June 1959. (Unpublished.)
19.* Ray W. Fisher and Charles W. Fullhart, Feasibility Studies on Molten Metal Reactor Components, A/CONF.15/P/1032.
20. Semi-Annual Summary Research Report in Engineering for July–December 1958, ISC-1118, Apr. 15, 1959. (Unclassified AEC report.)
21. W. W. Parkinson and O. Sisman, Liquid Metal Loops Irradiated in the ORNL Graphite Reactor and the LITR, ORNL-2630, June 1, 1959. (Unclassified AEC report.)
22. "Liquid Metals and Solidification," American Society for Metals, 1958.
23. J. C. Clark and W. J. Zager, Iron-Aluminum Alloy Systems, Part 2: Some Investigations in Air-Melting and Applications of Iron-Aluminum Alloys, WADC-TR-57-298(Pt. 2), May 1957. (Unclassified USAF report.)
24. F. Tate, Development of Iron–Aluminum-base Alloy for Gas-cooled Reactor Components, MND-DB-2525, April 1959. (Unclassified AEC report.)
25. Army Gas-cooled Reactor Systems Program, Monthly Progress Report, IDO-28538, Apr. 30, 1959. (Unclassified AEC report.)
26. R. Darras, Corrosion Problems in Gas-cooled Reactors, *Bulletin d'informations scientifique et technique*, 21: 13-25 (1958), IGIS-8(RD/W). Translated by P. J. Robinson (U. K. A. E. A., Sellafield).
27. Metallurgical Development for Hanford Program, Reaction of Yttrium with Water Vapor, ISC-1144, Apr. 15, 1959. (Unclassified AEC report.)
28. V. N. Konev, I. S. H. Trakhtenberg, and S. V. Shumilina, The Oxidation of Chromium in Air and in Oxygen, *The Physics of Metals and Metallography*, 5(1): 190-191 (1957).
29. Chemical Engineering Division Summary Report for January, February, and March 1959, ANL-5996, June 1959. (Unclassified AEC report.)
30. S. J. Rodgers and G. E. Kennedy, Fission-product Release During a Simulated Meltdown of a PWR Type Core, Mine Safety Appliances TR-63, Oct. 20, 1958, MSA Research Corp.
31. C. R. Houska and B. L. Averbach, Neutron Irradiation Effects in a Copper-Aluminum Alloy, AECU-4018, 1958. (Unclassified AEC report.)
32. J. A. Brinkman, Production of Atomic Displacements by High-energy Particles, *American Journal of Physics*, 24(4): 246-267 (April 1956).
33. P. Sagalyn, Use of Nuclear Magnetic Resonance for Radiation Effect Studies, MRL-36, July 1958, Materials Research Laboratory.
34. J. M. Davidson, E. M. Woodruff, and H. H. Yoshikawa, High-temperature Radiation-induced Graphite Contraction, HW-57900(Rev.), Feb. 2, 1959. (Unclassified AEC report.)
35. Irving B. Cadoff, A Literature Survey on the Relationship Between Dimensional Changes Produced by Radiation and Crystal Structure, WADC-TR-58-325, June 1958. (Unclassified USAF report.)
36. S. F. Pugh, Part I. Possible Effects of Irradiation in a Nuclear Reactor on the Properties of Steel, AERE M/M-219, January 1959. (Unclassified British report.)
37. W. O. Schaffnit, Radiation Damage Studies of Boron Stainless Steel, IDO-16502, Jan. 28, 1959. (Unclassified AEC report.)
38. Zirconium Highlights, WAPD-ZH-16, April 1959. (Unclassified AEC report.)
39. R. S. Kemper and D. L. Zimmerman, Neutron Irradiation Effects on the Tensile Properties of Zircaloy-2, HW-52323, Aug. 22, 1947. (Unclassified AEC report.)
40. L. M. Howe and W. R. Thomas, The Effect of Neutron Irradiation on the Tensile Properties of Zircaloy-2, CR-MET-827 (AECL-809), March 1959. (Unclassified Canadian report.)
41. Fundamental and Applied Research and Development in Metallurgy, Progress Report for February 1959, NMI-2075, Mar. 30, 1959. (Secret AEC report.)
42. Zirconium Highlights, WAPD-ZH-15, March 1959. (Unclassified AEC report.)
43. Lee E. Tanner and Charles R. Simcoe, Studies of Zirconium-Iron-Tin Alloys, ARF-2068-6, Apr. 30, 1959. (Unclassified AEC report.)
44. Semi-Annual Summary Research Report in Metallurgy for January to June 1958, ISC-1050, Mar. 1, 1959. (Unclassified AEC report.)
45. I. P. Bell, United Kingdom Atomic Energy Authority, May 18, 1955. (Unpublished.)
46. R. D. Stacey, Some Primary Phases in the Magnesium-Aluminum-Calcium System, RDB(S)TN-2167, 1958. (Unclassified British report.)
47. P. Shewon, Diffusion in Metals, *Industrial and Engineering Chemistry*, 51: 402-405 (March 1959).
48. Fundamental and Applied Research and Development in Metallurgy, Progress Report for January 1959, NMI-2074, Mar. 9, 1959. (Secret AEC report.)
49. R. W. Swindeman and D. A. Douglas, Improvements of the High-temperature Strength Properties of Reactor Materials after Fabrication, ORNL-2687, June 15, 1959. (Unclassified AEC report.)
50. J. J. Keys, Jr., and A. I. Krahoviak, High-frequency Surface Thermal Cycling of Inconel at 1400°F, *Transactions of the American Nuclear Society*, 2(1): (June 1959).
51. D. A. Roberts, D. B. Roach, and A. M. Hall, Physical and Mechanical Properties of Nine

Commercial Precipitation-Hardenable Stainless Steels, DMIC-112, May 1, 1959, Battelle Memorial Institute.

52. F. R. Schwartzberg, H. R. Ogden, and R. I. Jaffee, Ductile-Brittle Transition in the Refractory Metals, DMIC-114, June 25, 1959, Battelle Memorial Institute.

53. L. G. Bell, Creep and Tensile Properties of Magnesium Alloy AZ-61 at 50°C, CR-MET-824 (AECL-779), December 1958. (Unclassified Canadian report.)

*Second United Nations International Conference on the Peaceful Uses of Atomic Energy, Geneva, September 1958. (Individual papers are available from the Office of Technical Services, Dept. of Commerce, Washington 25, D. C. Bound volumes of papers are available from United Nations, Office of Public Information, New York.)

## *Melting, Casting, Heat-treatment, and Hot Working*

Mallinckrodt workers are investigating the practicability of reducing the hydrogen content of dingot metal to below 2.0 ppm by vacuum pouring.[1] Difficulties initially encountered with the establishment and maintenance of a vacuum seal between the mold and reduction container and in obtaining a reliable method of pouring have been overcome. No appreciable carbon pickup from the graphite mold was noted; however, the potential of the process has not been realized, and continuing efforts are planned in three specific areas. These relate to (1) the effect of pouring time (how long and at what point in the reduction cycle) on yield and ingot-surface quality, (2) the effect of the pressure maintained in the mold chamber on the hydrogen reduction effected, and (3) the effect of mold configuration on the surface quality of the ingot.

Interest in the reduction in the quantity of carbon picked up by uranium during melting continues. Hanford found that flame-sprayed zirconia is superior to other crucible materials in maintaining the low carbon content of as-reduced uranium; 30 to 50 ppm is obtained for uranium held 30 min at 1475°C. Magnesium zirconate was also found to be fairly successful, confirming the results previously reported by National Lead.[2] The importance of the method of application of the mold coating was demonstrated by both Hanford and National Lead. A zirconia coating, found to be best when flame sprayed, was poor when it was applied either as a butyl-alcohol slurry or applied and subsequently reacted in vacuum with the crucible before use.

An examination of the factors involved in the solidification of cylindrical uranium ingots has been made by Battelle.[3] Through theoretical study and experimental observation, a mathematical model was developed. Good correlation of the results (from computer runs) predicted by the mathematical model with data obtained during the casting of large ingots has been shown. The mathematical model is being used to evaluate variations in superheat, mold preheat, time of pour, and emissivity changes in the outer mold wall.

Interest in metallic materials for high-temperature service remains high. The Defense Materials Information Center has published in memorandum form H. Goodwin's remarks dealing with the current interest in molybdenum, titanium, and zirconium.[4] The forging of each metal is discussed, each metal is reviewed briefly, and the effect of the metallurgical characteristics on forging practice is explained; and practical hints are included.

In a recent study[5] the compatibility of various molybdenum-base alloys with existing process equipment was evaluated. The materials were prepared by arc melting in helium atmospheres and in vacuum and were fabricated by extrusion, forging, and rolling. The materials so produced were evaluated for soundness, forgeability, machinability, and hot hardness. The fabricated bar stock was further studied with regard to its recrystallization temperature, grain growth and embrittlement characteristics, tensile and creep properties, and brittle-to-ductile transition temperature. Under the conditions imposed, some alloys cracked on cooling after alloying in the arc furnace. On the basis of strength, corrosion, and recrystallization, the best alloy of the 17 evaluated contained 0.40 wt.% titanium, 0.08 wt.% zirconium, and 0.08 wt.% carbon. The alloy required 1 hr at 2950°F for complete recrystallization. Further, at 1800°F for 100 hr it exhibited a rupture stress of 79,000 psi; this was 9000 psi above that exhibited by the next best material. Applied stresses were found to increase the tendency for recrystallization to occur at elevated temperatures. (E. L. Foster)

## *Cladding*

### Cladding by Roll Bonding and Swaging

The high-temperature strength of iron-aluminum makes it a desirable cladding material for high-temperature gas-cooled-reactor fuels. An investigation of the self-bonding of various iron-aluminum alloys by roll bonding was made at Martin.[6] Coupons for this self-bonding study were prepared from 0.080- by 1- by 3-in. plates of iron-aluminum alloy that were abraded and fusion edge welded to form composite specimens. The most significant problem encountered in obtaining a complete bond was the presence of oxide formed on the mating surfaces. This oxide must be broken up during rolling to obtain a fresh clean surface for self-bonding. Roll-cladding temperatures of 1800 to 2200°F were employed in this study, with reductions of 60 per cent on the initial pass producing the best bonds. Smaller initial reductions or surface contamination resulted in weak bonds.

Hanford is investigating the Zircaloy cladding of fuel-element rods by hot swaging. Formerly, serious cracking or end effects were observed in the Zircaloy during cladding by hot swaging; however, recent experiments have demonstrated that, by reducing the "throw" of the dies on a stationary-spindle swaging machine, improved fabrication properties are obtained. (Edwin S. Hodge)

### Pressure Bonding

A process utilizing relatively high gas pressures and temperatures is being investigated for the cladding and joining of fuel elements and assemblies. The gas pressure forces components to be bonded into the initmate contact that is necessary for solid-phase diffusion to occur. Bonding is achieved with essentially no deformation; consequently the process is especially suited to the cladding and bonding of brittle fuel materials, high-temperature materials, and fuel systems composed of core and cladding that possess dissimilar fabrication properties.

Sylvania[7] is investigating the use of gas-pressure bonding for the simultaneous densification and cladding of $UO_2$ with stainless steel. The cold-pressing characteristics of different types of $UO_2$ and the effects of variation of $UO_2$ particle size and compacting pressure have been determined. Densities of up to 80 per cent of the theoretical density have been achieved by cold pressing, and densities of up to 98 per cent have been achieved by subsequent gas-pressure bonding at 1250°C with a gas pressure of 12,000 psi.

A similar study involving the simultaneous densification and cladding of ceramic, cermet, and dispersion fuels has been initiated at Battelle.[3,8,9] For $UO_2$ ceramic fuels the effects of $UO_2$ particle size, stoichiometry, porosity, and microstructure on the initial cold-pressed density are being determined. Both rod and flat-plate fuel elements are being pressure bonded. A small stainless-steel-clad $UO_2$ fuel assembly has been bonded in one operation to establish the feasibility of preparing complete fuel assemblies by this process.

The use of the gas-pressure-bonding process is being investigated[3,8,9] for the preparation of Zircaloy-clad flat-plate uranium dioxide fuel elements. The $UO_2$ fuel is compartmented with Zircaloy strips for structural strength and to form individual gastight compartments capable of retaining released fission gas with a minimum of cladding deformation. The process, as established, consists of the assembly of belt-abraded components to form the compartmented picture frame. Zircaloy covers are applied, and the assembly is fusion edge welded to form a gastight envelope. Bonding is achieved at 1550°F for 4 hr with a helium-gas pressure of 10,000 psi. The pressure-bonded elements have been tested by Bettis and found to exhibit normal behavior and satisfactory bond integrity.[10]

The bonding of niobium and molybdenum fuel systems is also being studied.[3,8,9] Techniques have been developed for the self-bonding of niobium. The bonds possess complete grain growth across the interface, high strength, and excellent ductility. In order to eliminate reaction with container materials, the niobium is bonded in a two-step operation. In the initial step, a gastight assembly is formed by brazing the niobium components together with zirconium at 1650°F. This gastight assembly is then bonded at 2100°F for 3 hr with a gas pressure of 10,000 psi.

A study is being conducted at Battelle[3,8,9] with the objective of establishing the kinetics and mechanism of solid-state bonding as achieved by the use of heat and pressure. The bond line formed by pressure bonding resembles a grain boundary; however, it does not appear to behave as a normal grain boundary. Frequently after annealing, pinhole porosity is detected at the

bond line. Diffusion studies have been initiated to determine whether the rate of diffusion is more rapid along the bond line than it is along a normal grain boundary. (S. J. Paprocki)

## Diffusion Bonding

The effects of welding temperature, welding time, total upset, and welding stress on the bond strengths between Zircaloy-2 and uranium-zirconium alloys were investigated by Bettis. Bonded specimens were prepared by pressure welding the two materials *in vacuo* with an apparatus designed for control and measurement of pressure-welding variables. Shear testing was found to be the most useful method of evaluating the effects of these variables on the weld strength. Mechanical testing was correlated with optical and electron microscopy observations. These experiments indicated that a relation may exist between the relative shear strengths of the welded couples and the occurrence of a nearly continuous layer of particles at the uranium-rich side of the diffusion zone. Also, the welding temperature was the most significant variable for Zircaloy-2 to uranium-zirconium welds. Zircaloy-2 was found to bond more readily to both uranium-base alloys than did Zircaloy-3. When the component surfaces were contaminated by oxide or contaminants from within the pressure-welding apparatus, incomplete bonding of the welding couples resulted.

Two eutectic diffusion-bonding methods for fabricating Zircaloy-clad compartmented plate type $UO_2$-bearing fuel elements are being investigated at Bettis. Both methods involve the formation of a molten eutectic-alloy film between the solid mating surfaces to be joined. The eutectic-alloy film is formed by diffusion of a thin preplaced layer of pure metal (iron or copper) on the adjacent surfaces during heating of the assembled components. Improved control in the chemical plating of copper on Zircaloy by dynamic flow conditions has been demonstrated with the use of new equipment.[10] The assembled components are sealed prior to bonding by fusion welding along the outside periphery of the assembly. One method involves the application of a small positive inert-gas pressure to the external cladding surfaces during the bonding operation.

An investigation of copper-diffusion bonding in pressurized-liquid salt baths was initiated with promising results. It was found that the heating rate is about 20 times faster than that realized in gas bonding, and therefore the excessive diffusion of copper is avoided before reaching the bonding temperature. It was also found that the cooling rate is 10 times faster than the minimum required to retain good cladding corrosion resistance, which is another advantage of salt bonding over gas bonding. Bonds similar to those obtained in gas bonding are indicated by microscopic examination and by internal-pressure burst tests. Mechanical-property tests and the effect of salt bonding on contamination of Zircaloy and the resultant corrosion properties are being investigated. Initial results indicate that the bath must be gettered to remove oxygen and water vapor. Techniques for doing this have been highly successful. Contamination by the salt itself is minor and has not affected corrosion resistance in short-time tests in 680°F water. (M. A. Gedwill, Jr.)

## Coextrusion

Investigations were made by Nuclear Metals[11] to obtain beryllium cladding heavier than 15 mils on long coextruded rods of uranium–2 wt.% zirconium. The objectives were to obtain test rods which would allow cladding thickness to be a variable in the testing program.

Three coextrusions of $UO_2$ cold compacted at 10,000 psi in 1-in.-OD, 16-gauge sleeves of type 304 stainless steel have been accomplished by Nuclear Metals.[12–14] Examination of each of the rods revealed dog boning and cracking of the $UO_2$, as well as a lack of uniformity in the stainless-steel cladding thickness. The oxide had not flowed plastically, as had been observed in an earlier extrusion made under similar conditions.

A flat rod of Zircaloy-2-clad uranium–2 wt.% zirconium approximately $\frac{1}{4}$ by $\frac{7}{8}$ in. in cross section was extruded from a 2-in.-diameter billet by Nuclear Metals.[14] This rod was sectioned in the region of the extruded end closures and examined. There appeared to be very little thinning of the cladding at the beginning of the end seal, and the thickness of the cladding was very uniform in the center portion all around the perimeter. This favorable result was unexpected since earlier attempts at extruding clad flats had always led to marked thickening of the cladding at the edges. (C. B. Boyer)

### Canning

Vibratory packing of fissile ceramic fuel to moderate densities in cladding tubes offers the possibility of a simple means of fuel-element fabrication. Ground fused and PWR type $UO_2$ powders were compacted to 86 and 46.5 per cent of the theoretical density, respectively, by vibratory compaction in 44.75-in.-long, 0.57-in.-diameter Zircaloy tubes. The test was performed on a 500-lb thrust, 5 to 5000 cps, Genisco-Savage vibrator driven by a 1-kw amplifier. The stated densities were achieved in less than 1 min of vibration at 33 g at the resonant frequencies of the tubes, which varied from an initial 220 cps to 280 cps at maximum compaction.

A complete history of development and methods used in each step of the cleaning, assembling, and canning in the Hanford lead-dip process is given in reference 15.

(Paul H. Bonnell)

### Nonelectrolytic Chemical-plating Techniques

Attempts at Battelle[16] to obtain protection with pure silicon carbide confirmed the conclusion that a layer of elemental silicon is essential to the oxidation resistance of the composite. Heating of graphite at 2000°C in a mixed $SiI_4$-$SiBr_4$ atmosphere produced a spongy layer of silicon carbide. It is suggested that this be used to form the matrix for a protective film of liquid silicon, which can be deposited by eliminating $SiBr_4$ from the mixture and dropping the temperature to 1450°C or by dipping in liquid silicon.

Pyrolysis of methane at 1000°C was used at Battelle[3,8,9] to coat $UO_2$ fuel cores with several microinches of hard carbon. Chromium coatings were applied to cores by vacuum evaporation and by hydrogen reduction of an occluded film of liquid chromous iodide.

(J. M. Blocher, Jr.)

### Ceramic Coatings

Ames Laboratory[17] reports that a porcelain-enamel type of coating has been found which has a low thermal-neutron cross section and which will protect yttrium against oxidation in air at 800°C, provided the coating is free of defects.

The Defense Metals Information Center[18] has issued a memorandum describing glass-bonded refractory coatings to prevent corrosion or to provide thermal insulation for iron- or nickel-base alloys. Compositions as well as details of metal preparation and coating application are given.

• A U. S. patent[19] has been granted on a ceramic coating composed of CaO, $Al_2O_3$, and $SiO_2$ for protecting a beryllium carbide–graphite body.

(B. W. King)

## *Welding and Brazing*

A program to study ceramic-coated backing in the welding of Zircaloy fuel assemblies is being conducted by Babcock & Wilcox for Knolls. The program will establish: (1) the corrosion resistance of Zircaloy welds made with carbon-steel backing faced with $ZrO_2$, (2) the feasibility of using a $ZrO_2$-coated Ti-Namel spacer for molding a water-channel radius, and (3) the feasibility of welding sections with $UO_2$-coated Ti-Namel spacers. Results up to now show that corrosion behavior is not adversely affected unless excessive heat input causes the pickup of $ZrO_2$ particles. Little success has been obtained in using a backup to mold the water-channel radius, and contoured backups are now being studied.

A study of methods for end capping zirconium-clad reactor fuel pins is reported by personnel from Battelle.[20] Resistance-upset butt welding, mechanical attachment, and inert-gas-shielded tungsten-arc welding were investigated thoroughly. Recessed-core fuel pins, to receive an end-cap insert that is attached and sealed by arc welding, produced the best seal.

(R. E. Monroe)

## *Nondestructive Testing*

Standard ultrasonic, eddy-current, and radiographic methods are still the basic methods being used to nondestructively test nuclear components. The application of these methods to specific problems[14,21–25] has resulted in a steady advance of the art so that the exacting demands for high integrity in nuclear components are being met on a wide front.

Two techniques stand out as the most promising for future developments. These are gamma-scintillation techniques and X-ray fluorescence photometers. Both can be applied on a wide

variety of materials and shapes. The X-ray photometer, although limited in its applicability, appears capable of a very high degree of precision. (C. V. Weaver)

## *References*


1. D. E. Treadway and B. J. Buntz, in Process Development Quarterly Report. Part II. Pilot Plant Work, MCW-1429, May 1, 1959. (Confidential AEC report.)
2. O. Magoteaux, D. L. Elston, and C. F. Hall, Laboratory Evaluation of Graphite Crucible Coatings for Vacuum Melting Uranium, NLCO-759, Oct. 24, 1958. (Unclassified AEC report.)
3. R. W. Dayton and C. R. Tipton, Jr., Progress Relating to Civilian Applications During June 1959, BMI-1357, July 1, 1959. (Unclassified AEC report.)
4. Harry B. Goodwin, Some Metallurgical Considerations in Forging Molybdenum, Titanium, and Zirconium, DMIC-Memo-12, Mar. 25, 1959, Battelle Memorial Institute.
5. M. Semchyshen, Gordon D. McArdle, and Robert Q. Barr, Development of High Strengths and High Recrystallization Temperatures in Molybdenum-base Alloys, WADC-TR-58-551, February 1959. (Uncalssified USAF report.)
6. Frank Tate, Development of Iron-Aluminum Alloys for Gas-cooled Reactor Components, MND-DB-2525, April 1959. (Unclassified AEC report.)
7. L. W. Kates, in Quarterly Technical Progress Report for Period Ending March 31, 1959, SCNC-296, May 1959. (Confidential AEC report.)
8. R. W. Dayton and C. R. Tipton, Jr., Progress Relating to Civilian Applications During April 1959, BMI-1340, May 1, 1959. (Unclassified AEC report.)
9. R. W. Dayton and C. R. Tipton, Jr., Progress Relating to Civilian Applications During May 1959, BMI-1346, June 1, 1959. (Confidential AEC report.)
10. Pressurized Water Reactor (PWR) Project Technical Progress Report for the Period February 24, 1959, to April 23, 1959, WAPD-MRP-79, May 1959. (Unclassified AEC report.)
11. Fundamental and Applied Research and Development in Metallurgy, Progress Report for February 1959, NMI-2075, Mar. 30, 1959. (Secret AEC report.)
12. Fundamental and Applied Research and Development in Metallurgy, Progress Report for March 1959, NMI-2076, May 13, 1959. (Secret AEC report.)
13. Fundamental and Applied Research and Development in Metallurgy, Progress Report for January 1959, NMI-2074, Mar. 9, 1959. (Secret AEC report.)
14. F. S. Gardner et al., Power Reactor Program, Progress Report to E. I. du Pont de Nemours and Company for the Period January 1, 1959, Through January 31, 1959, NMI-4385, Feb. 26, 1959. (Unclassified AEC report.)
15. E. A. Weakley, Technology of the HAPO Lead Dip Fuel-element Canning Process, HW-58115, Dec. 15, 1958. (Confidential AEC report.)
16. J. M. Blocher, Jr., D. P. Leiter, Jr., and R. P. Jones, Coating of Graphite with Silicon Carbide by Reaction with Vapor of Controlled Silicon Activity, BMI-1349, June 15, 1959. (Unclassified AEC report.)
17. Semi-Annual Summary Research Report in Engineering for July–December 1958, ISC-1118, Apr. 15, 1959. (Unclassified AEC report.)
18. T. E. Cook and B. W. King, Glass-bonded Refractory Coatings for Iron- or Nickel-base Alloys, DMIC-Memo-16, Apr. 25, 1959, Battelle Memorial Institute.
19. M. K. Blanchard, Composition and Method for Coating a Ceramic Body, U. S. Patent 2,858,138, Nov. 4, 1958.
20. J. J. Vagi, R. L. Koppenhoffer, and D. C. Martin, Methods for End Capping Zirconium-clad Reactor Fuel Pins, *Welding Journal*, 38(2): 78s-84s (February 1959).
21. Papers Presented at the Reactor Fuel Measurement Symposium, TID-7560, June 18–20, 1958. (Unclassified AEC report.)
22. W. N. Beck et al., Nondestructive Testing of EBR-I Mark III Fuel Elements and Components, ANL-5893, May 1959. (Unclassified AEC report.)
23. E. G. Stanford and J. H. Fearon, eds., "Progress in Nondestructive Testing," Heywood and Company, Ltd., Vol. 1, 1958.
24. John W. Allen, Eddy-Current Testing in Practice, ORNL-2655, Apr. 30, 1959. (Unclassified AEC report.)
25. S. Priceman, Quantitative Determination of Uranium Loading of Aluminum-clad Fuel Plates by X-ray Densitometry, SCNC-277, October 1958. (Unclassified AEC report.)

## LEGAL NOTICE

This document was prepared under the sponsorship of the U. S. Atomic Energy Commission. Neither the United States, nor the Commission, nor any person acting on behalf of the Commission:

A. Makes any warranty or representation, expressed or implied, with respect to the accuracy, completeness, or usefulness of the information contained in this report, or that the use of any information, apparatus, method, or process disclosed in this report may not infringe privately owned rights; or

B. Assumes any liabilities with respect to the use of, or for damages resulting from the use of any information, apparatus, method, or process disclosed in this report.

As used in the above, "person acting on behalf of the Commission" includes any employee or contractor of the Commission, or employee of such contractor, to the extent that such employee or contractor of the Commission, or employee of such contractor prepares, disseminates, or provides access to, any information pursuant to his employment or contract with the Commission, or his employment with such contractor.

# NUCLEAR SCIENCE ABSTRACTS

The U. S. Atomic Energy Commission, Technical Information Service, publishes *Nuclear Science Abstracts (NSA)*, a semimonthly journal containing abstracts of the literature of nuclear science and engineering.

*NSA* covers (1) research reports of the U. S. Atomic Energy Commission and its contractors; (2) research reports of government agencies, universities, and industrial research organizations on a world-wide basis; and (3) translations, patents, books, and articles appearing in technical and scientific journals.

Complete indexes covering subject, author, source, and report number are included in each issue. These are cumulated quarterly, semiannually, and annually providing a detailed and convenient key to the literature.

## Availability of *NSA*

**SALE** *NSA* is available on subscription from the Superintendent of Documents, U. S. Government Printing Office, Washington 25, D. C., at $18.00 per year for the semimonthly abstract issues and $15.00 per year for the four cumulated-index issues. Subscriptions are postpaid within the United States, its Territories, Canada, Mexico, and all Central and South American countries, except Argentina, Brazil, British and French Guiana, Surinam, and British Honduras. Subscribers in these Central and South American countries, and in all other countries throughout the world, should remit $22.50 per year for subscriptions to semimonthly abstract issues and $17.50 per year for the four cumulated-index issues.

**EXCHANGE** *NSA* is also available on an exchange basis to universities, research institutions, industrial firms, and publishers of scientific information. Inquiries should be directed to the Technical Information Service Extension, U. S. Atomic Energy Commission, P. O. Box 62, Oak Ridge, Tennessee.

*REACTOR CORE MATERIALS* may be purchased ($2.00 per year, $0.55 per issue) from the Superintendent of Documents, U. S. Government Printing Office, Washington 25, D. C. The use of the coupon below will facilitate the handling of your order.

POSTAGE AND REMITTANCE: Postpaid within the United States, its Territories, Canada, Mexico, and all Central and South American countries except as hereinafter noted. Add $0.50 per year, or $0.15 per single issue, for postage to all other countries, including Argentina, Brazil, British, Dutch, and French Guiana, and British Honduras. Payment should be by check, money order, or document coupons, and MUST accompany order. Remittances from foreign countries should be made by international money order, or draft on an American bank, payable to the Superintendent of Documents, or by UNESCO book coupons.

## *order form*

SUPERINTENDENT OF DOCUMENTS
U. S. GOVERNMENT PRINTING OFFICE
WASHINGTON 25, D. C.

Enclosed:
document coupons ☐ check ☐ money order ☐

Charge to Superintendent of Documents No. _____

Please send me a one-year subscription to

REACTOR CORE MATERIALS
($2.00 a year; $0.55 per issue.)

SUPERINTENDENT OF DOCUMENTS
U. S. GOVERNMENT PRINTING OFFICE
WASHINGTON 25, D. C.

(Print clearly)

Name _____

Street _____

City _____ Zone____State _____